LAND–ATMOSPHERE INTERACTIONS

The LoCo Perspective

Joseph A. Santanello Jr., Paul A. Dirmeyer, Craig R. Ferguson, Kirsten L. Findell, Ahmed B. Tawfik, Alexis Berg, Michael Ek, Pierre Gentine, Benoit P. Guillod, Chiel van Heerwaarden, Joshua Roundy, and Volker Wulfmeyer

Metrics derived by the LoCo working group have matured and begun to enter the mainstream, signaling the success of the GEWEX approach to foster grassroots participation.

The role of land–atmosphere (L-A) interactions in weather and climate prediction has emerged over the last two decades as important but inherently challenging and complex. One reason is that L-A interaction research has proceeded "in reverse" compared to most science. Typically in Earth system sciences, observations inform theory, which then leads to the development and gradual refinement of conceptual and numerical models based on elucidated physical processes. The benchmark for such models' success, and the progress of the underlying science, is when they begin to consistently outperform purely statistical approaches inherently not based in the representation of physical processes (Best et al. 2015).

Conversely, coupled L-A (i.e., weather and climate) models arose well before the theoretical basis for

AFFILIATIONS: Santanello—Hydrological Sciences Laboratory, NASA Goddard Space Flight Center, Greenbelt, Maryland; Dirmeyer—Center for Ocean–Land–Atmosphere Studies, George Mason University, Fairfax, Virginia; Ferguson—Atmospheric Sciences Research Center, University at Albany, State University of New York, Albany, New York; Findell—Geophysical Fluid Dynamics Laboratory, Princeton, New Jersey; Tawfik—National Center for Atmospheric Research, Boulder, Colorado; Berg—Department of Civil and Environmental Engineering, Princeton University, Princeton, New Jersey; Ek—National Centers for Environmental Prediction, College Park, Maryland; Gentine—Earth and Environmental Engineering, Columbia University, New York, New York; Guillod—Institute for Environmental Decisions, and Institute for Atmospheric and Climate Science, ETH Zurich, Zurich, Switzerland; van Heerwaarden—Meteorology and Air Quality Group, Wageningen University, Wageningen, Netherlands; Roundy—Civil, Environmental and Architectural Engineering, University of Kansas, Lawrence, Kansas; Wulfmeyer—Institute of Physics and Meteorology, University of Hohenheim, Stuttgart, Germany
CORRESPONDING AUTHOR: Dr. Joseph A. Santanello Jr., joseph.a.santanello@nasa.gov

The abstract for this article can be found in this issue, following the table of contents.
DOI:10.1175/BAMS-D-17-0001.1

In final form 30 November 2017

L-A interactions had begun to mature, driven by the pressing need to supply accurate lower-boundary conditions to atmospheric models as their use was extended from weather time scales to seasonal and longer periods. Demand for closure of surface energy and water budgets in atmospheric models led to the development of the first land surface models (LSMs; e.g., Manabe 1969) that were internally consistent, but not necessarily well behaved when coupled to atmospheric models that often have strong precipitation or radiative energy biases over continents.

As was the case with early coupled ocean–atmosphere models, strong climate biases developed when LSMs were coupled to general circulation models (GCMs). But unlike the ocean, for which fairly comprehensive measurements of sea surface temperatures were available to expose the symptoms of coupled model biases, the land surface lacked routine observations of states like soil moisture and temperature, vegetation water content, and snow mass. In addition, key LSM parameters and state variables can be difficult to observe routinely, or are unmeasurable [e.g., soil moisture in models versus observations, as discussed in Koster et al. (2009)]. As a result, LSMs traditionally have lacked a full representation of components such as water transport (e.g., groundwater) and vegetation dynamics, and the method for correcting meteorological biases in weather and climate forecast models often falls to tuning relatively unconstrained LSM parameters, such as vegetation rooting depth, to compensate for atmospheric model shortcomings (Kleidon and Heimann 1998).

Over time, separate atmospheric and land surface model development communities have emerged. Although working toward related goals, the two communities have operated in parallel and have been largely unsuccessful in addressing coupled process representation via joint modeling efforts. As a result, the development and evaluation of traditional LSMs and hydrological models has occurred predominantly in an offline (uncoupled) mode (van den Hurk et al. 2011). The study of L-A interactions has emerged from a need to explore system feedbacks to improve process understanding and model performance. In this paper, we first outline the broader context of L-A interactions over time and the emergence of the Global Energy and Water Exchanges project (GEWEX) international community-based Local Land–Atmosphere Coupling (LoCo) initiative. The following sections discuss the evolution of LoCo over time and its contributions to the research community.

A BRIEF HISTORY OF L-A INTERACTION RESEARCH. It is widely accepted that realistically representing coupled processes in models is a prerequisite for surface climate predictability (Betts 2004). However, the necessary spatial and temporal coverage of observations to underpin coupled L-A model evaluation and development has been lacking (Guillod et al. 2014). The prototypical two-week field campaigns that have been the backbone of developing atmospheric process understanding have proved too short to provide the necessary data, and longer campaigns are costly. With few exceptions [e.g., the First International Satellite Land Surface Climatology Project (ISLSCP) Field Experiment (FIFE; Hall and Sellers 1995) and the Cooperative Atmosphere–Surface Exchange Study (CASES; Yates et al. 2001; Moeng et al. 2003)], the majority of campaigns are also lacking in terms of addressing the full suite of measurements (across the soil–vegetation–atmosphere system) required for L-A studies, focusing on observations in one or two of these compartments only. The new Land–Atmosphere Feedback Experiment (LAFE), which was conducted in August 2017, was designed to close these observational gaps (Wulfmeyer et al. 2018).

Additionally, land surface properties (e.g., land cover, terrain, and soil texture) are highly heterogeneous across a wide range of spatiotemporal scales, hampering generalization of measurements from one location to another. As a result, the multivariate and multiscale coupled L-A processes remain *poorly observed and incompletely understood* (e.g., Betts et al. 1996; Betts 2000, 2004; Ek and Holtslag 2004; Guo et al. 2006; Jimenez et al. 2014; Teuling et al. 2017). Standard model outputs, especially those from climate model intercomparison projects such as the Coupled Model Intercomparison Project (CMIP), are often insufficient to diagnose coupled sensitivities at the L-A interface.

Broadly speaking, the potential linkages between land surface variables such as soil moisture (SM) and atmospheric variables such as temperature or precipitation P are rather intuitive and have been highlighted in recent studies and review articles (e.g., Seneviratne et al. 2010; Betts and Silva Dias 2010). The importance of the land surface has been demonstrated not only in terms of predictability on daily to seasonal time scales (e.g., Koster et al. 2010; Hirsch et al. 2014; Dirmeyer and Halder 2016; Betts et al. 2017), but also in terms of influencing extremes such as drought and heatwaves (Roundy et al. 2013, 2014; Miralles et al. 2014; Wang et al. 2015; Pai Mazumder and Done 2016), planetary boundary layer (PBL) evolution and cloud formation (Milovac et al. 2016) and afternoon convection (Findell and Eltahir 2003a,b; Gentine et al. 2013a; Guillod et al. 2015), and tropical cyclone reintensification (Andersen and Shepherd 2014). Other linkages, such as the role of SM or vegetation heterogeneity in mesoscale circulations (e.g., Taylor et al. 2012; Hsu et al. 2017) and planetary waves (Koster et al. 2014), and those driven by land-use and land-cover change or management (e.g., Findell et al. 2007; Pitman et al. 2009; de Noblet-Ducoudré et al. 2012; Mahmood et al. 2014; Lejeune et al. 2015; Hirsch et al. 2015; Findell et al. 2017) are topics of active research. The fact that coupling studies are carried out across a range of time- and space-scale perspectives tends to also confound community thinking and consensus building (Guillod et al. 2015; Knist et al. 2017). For example, assessment of the coupling within GCMs may vary significantly from local diurnal scales to large and seasonal to interannual time scales (e.g., Wei et al. 2010; Ferguson et al. 2012; Green et al. 2017).

Understandably, the focus of the climate community in terms of L-A interactions has been on large-scale SM–*P* relationships and causality. Most notably, the Global Land Atmosphere Coupling Experiment (GLACE; Koster et al. 2004, 2006; Guo et al. 2006) highlighted potential regions where GCMs indicate the influence of antecedent SM on *P*, and the degree to which GCMs differ in describing that relationship (Dirmeyer et al. 2006). The GLACE studies highlighted the potential role of the land surface in climate predictability and served to galvanize community interest in L-A interactions, especially toward global hot spots of L-A coupling in many semiarid and agricultural areas. Since then, numerous studies have pursued the notion of coupling hot spots (e.g., Notaro 2008; Zhang et al. 2008; Anderson et al. 2009; Dirmeyer et al. 2009; Wei et al. 2010; Zeng et al. 2010; Zhang et al. 2011; Ferguson et al. 2012; Mei and Wang 2012). GLACE also exposed the need to revisit the complex interactions, controls, and feedbacks inherent to SM–*P* feedbacks that are indiscernible using

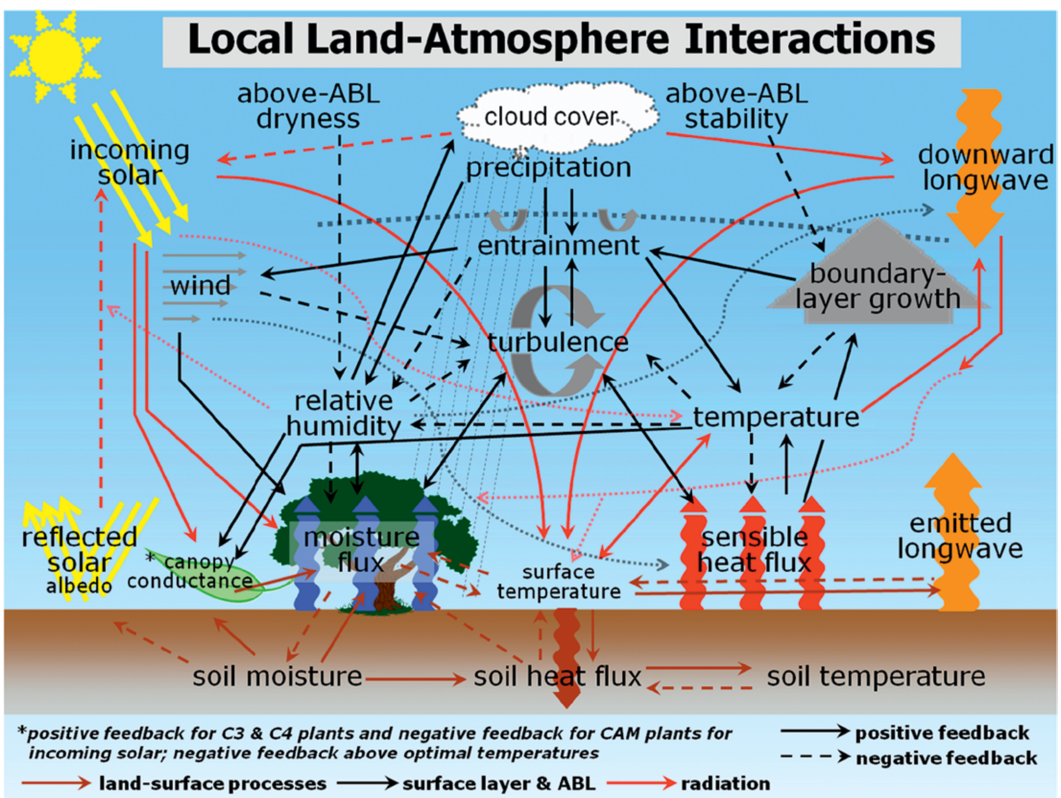

Fig. 1. A schematic of local L-A interactions in a quiescent synoptic regime, including the SM–*P* feedback pathways. Solid arrows indicate a positive feedback pathway and large dashed arrows represent a negative feedback, while red indicates radiative, black indicates surface layer and PBL, and brown indicates land surface processes. Thin red and gray dashed lines with arrows represent positive feedbacks. The single horizontal gray dotted line (no arrows) indicates the top of the PBL, and the seven small vertical dashed lines (no arrows) represent precipitation. Courtesy of M. Ek, embellished from earlier versions appearing in Ek and Mahrt (1994) and Ek and Holtslag (2004).

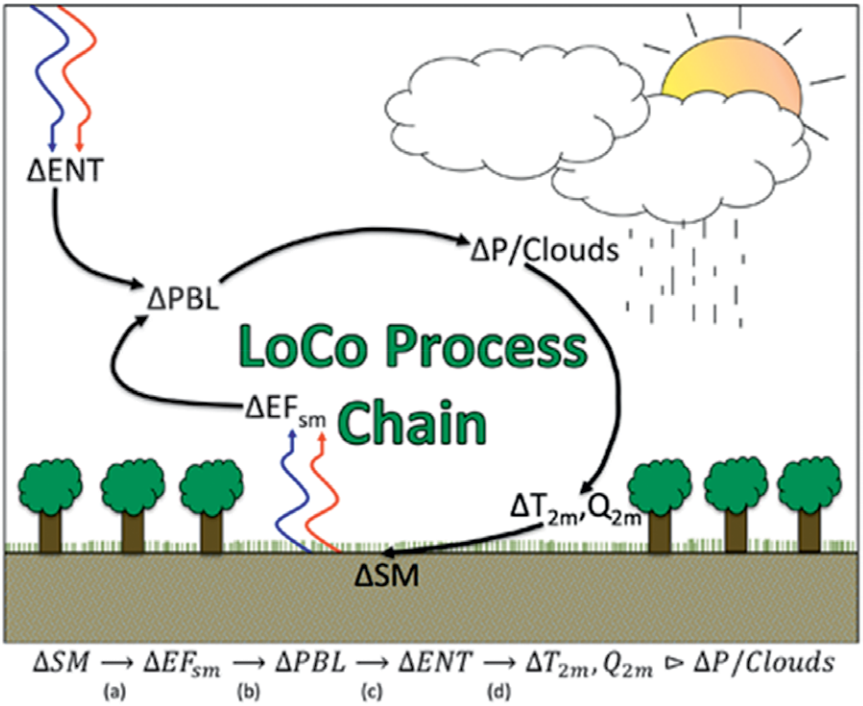

Fig. 2. Schematic of the LoCo process chain describing the components of L-A interactions linking soil moisture to precipitation and ambient weather (T_{2m}, Q_{2m}), where SM represents soil moisture; EF_{sm} is the evaporative fraction sensitivity to soil moisture; PBL is the PBL characteristics (including PBL height); ENT is the entrainment flux at the top of the PBL; T_{2m} and Q_{2m} are the 2-m temperature and humidity, respectively; and *P* is precipitation.

metrics that rely on large-scale ensemble statistics rather than observable features.

EVOLUTION OF LOCO. Over the last decade, the importance of L-A coupling for weather and climate model development has become more apparent under the GEWEX Imperatives (www.gewex.org/about/science/seven-gewex-imperatives) and the World Climate Research Programme (WCRP) Grand Challenges (www.wcrp-climate.org/grand-challenges/grand-challenges-overview). The overarching goals of these programs suggest that science must integrate approaches to evaluate atmospheric or land models to achieve further breakthroughs in model development and that comprehensive coupling metrics (rooted in observable process-level scales) should be integral to the model development cycle.

GLACE was an early element of the GEWEX Global Land–Atmosphere System Study (GLASS; van den Hurk et al. 2011), which was conceived as a voluntary, community-based panel under GEWEX in the late 1990s and focused on coordinating research efforts to evaluate and compare L-A models in four modes: 1) local-scale offline (i.e., uncoupled LSMs at the point scale), 2) large-scale offline (which have evolved into continental and global land data assimilation systems), 3) local-scale coupled (LSMs coupled to single-column models), and 4) large-scale coupled (LSMs coupled to GCMs) models. These have been addressed through community-supported model intercomparison projects (MIPs), including the Project for the Intercomparison of Land-Surface Parameterization Schemes (PILPS; Henderson-Sellers et al. 1993, 2002), the Global Soil Wetness Project (GSWP; Dirmeyer 2011a), and the aforementioned GLACE (Koster et al. 2006, 2010; Guo et al. 2006; Seneviratne et al. 2013; van den Hurk et al. 2012). However, formation of a local-scale coupled MIP (mode 3) has lagged, initially due to the difficulty both in selecting sufficiently holistic metrics and designing an experiment that incorporates the full complexity of local L-A interactions (Fig. 1). Note that PILPS and GSWP were performed in offline mode without atmospheric feedbacks (i.e., uncoupled), while GLACE, despite being a multimodel coupled experiment, lacked process-level diagnosis.

To address this, the GLASS-supported working group LoCo was established in the mid-2000s to coordinate and promote process-level, local L-A coupling research and develop integrative metrics to quantify these complex relationships and feedbacks. Over the years, LoCo has grown to facilitate integrated model development and identify observational needs to better understand the complex nature of L-A interactions and their role in a changing climate.

When referring to water and energy cycle research, LoCo defines local coupling as "the impact of land surface states on the evolution of surface fluxes, the PBL, and free atmosphere, including clouds and precipitation, as well as positive and negative feedback mechanisms that modulate extremes" (Santanello et al. 2011b). This incorporates the notion that all interactions between land and atmosphere begin locally through the interface of the land surface and PBL (see Fig. 1). The LoCo process chain, a simplification of the complexities illustrated in Fig. 1, is shown schematically in Fig. 2 and written as (Santanello et al. 2011a,b)

$$\Delta \mathrm{SM} \underset{a}{\rightarrow} \Delta \mathrm{EF} \underset{b}{\rightarrow} \Delta \mathrm{PBL} \underset{c}{\rightarrow} \Delta \mathrm{Ent} \underset{d}{\rightarrow} \Delta T_{2\mathrm{m}}, Q_{2\mathrm{m}} \Rightarrow \Delta P, \mathrm{Cloud}. \quad (1)$$

The links (arrows a–d) in the current process chain describe the sensitivities of a) surface sensible (H) and latent (LH) heat flux partitioning [i.e., evaporative fraction; EF = LH/(LH + H)] to SM, b) PBL height evolution to surface fluxes, c) entrainment fluxes to PBL height evolution, and d) the collective feedback of the free atmosphere (through the entrainment zone) on PBL thermodynamics. Taken in full, these interactions (a–d) contribute toward the development of convective cloud and precipitation, outlining the pathways that define the SM–P relationship (Fig. 2). The importance of these processes and interactions have been documented individually (e.g., Pan and Mahrt 1987; Oke 1987; Diak 1990; Brubaker and Entekhabi 1996; Dolman et al. 1997; Peters-Lidard and Davis 2000; Betts and Viterbo 2005; Santanello et al. 2005, 2007; LeMone et al. 2010a,b; Gentine et al. 2013a,b). Within this chain, there are also numerous positive and negative feedback loops, which have been detailed by Santanello et al. (2007), van Heerwaarden et al. (2009), and Seneviratne et al. (2010).

The LoCo process chain is far from being all-inclusive and can be augmented in the future to account for terms such as radiation, snow, landscape type (e.g., desert, grassland, and tundra), canopy interception, large-scale convergence, and additional feedbacks such as those related to clouds (Fig. 1). In addition, the focus to date has been on daytime process and interactions with the convective PBL. Nevertheless, it provides a framework for simplifying the myriad process interactions into a manageable and measurable series of quantities. Within this definition and scope, LoCo has been working to develop metrics and global mappings that quantify the components of Eq. (1). Voluntary contributors to LoCo span several continents and include both government and academia, and research interests include regional to global modeling and weather to climate prediction scales.

LOCO CONTRIBUTIONS. Arguably the most prominent contribution of LoCo has been the continued development and promotion of quantifiable L-A coupling metrics to diagnose the land and PBL/precipitation coupling. Rather than common single-variable factors such as bias, root-mean-square error, or skill scores, where compensating errors are often hidden and causality is obscured, multivariate metrics can be used to quantify critical aspects of the L-A coupled system in models and observations, allowing for the exposure of model differences and deficiencies in a systematic fashion.

Metrics and their diagnostic nature can be categorized in several ways. Figure 3 illustrates the suite of LoCo-relevant metrics defined by their temporal scales of application (x axis), by the link(s) within the LoCo process chain [Eq. (1]) they encapsulate (y axis), and by their statistical versus process-based nature (gray solid and dashed outlines). Some metrics, such as those quantifying soil moisture effects on surface fluxes, cover two-component interactions, and others, such as those connecting soil moisture to precipitation, capture the totality of interactions. LoCo metrics can shed light

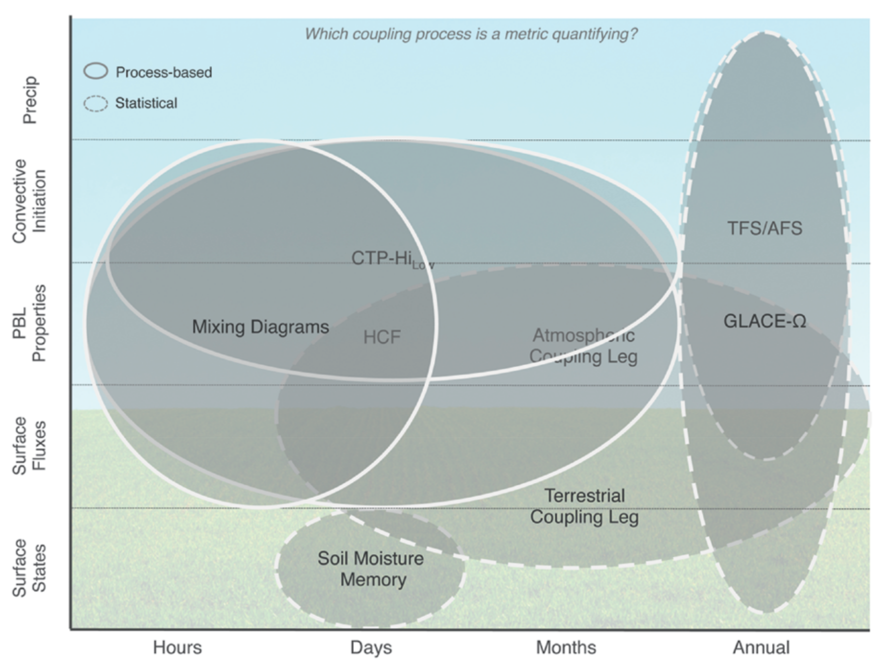

Fig. 3. LoCo metrics (see Table 1) across temporal scales (*x* axis), relationship to the LoCo process chain [Eq. (1)] along the *y* axis, and statistical vs process-based nature (elliptical outlines). Green background shading indicates land surface related states and fluxes, while blue indicates PBL and atmospheric variables.

TABLE 1. L-A coupling metrics portrayed in Fig. 3. A more thorough list of metrics and their descriptions is available at http://cola.gmu.edu/dirmeyer/Coupling_metrics.html.

Name of metric	Uses land states?	Uses surface fluxes?	Uses atmospheric states?	Strictly local in space?	Data time scale, period[a]	Calculate from observations?	Based on
Mixing diagrams	N	Y	Y	N[b]	Daytime	Y	2-m temperature and humidity evolution, surface fluxes, PBL depth
LCL deficit	N	N	Y	Y	Daytime	Y	2-m temperature, humidity, PBL depth
CTP–HI_{low}	N	N	Y	Y	Morning	Y	Temperature and humidity at specific atmospheric levels
HCF	N	Y	Y	Y	Any time of day	Y	Atmospheric profile, available energy at land surface
RH tendency	N	Y	Y	Y	Daytime	Y	Atmospheric profile, surface fluxes
Priestley–Taylor ratio	N	Y	Y	Y	Instantaneous or time means	Y	2-m temperature, humidity, surface fluxes
SMM	Y	N	N	Y	Daily or longer intervals	Y	Lagged autocorrelations of soil moisture
Terrestrial coupling leg	Y	Y	N	Y	Daily or longer means	Y	Variances and covariances of surface fluxes, land states
Atmospheric coupling leg	N	Y	Y	Y	Daily or longer means	Y	Variances and covariances of surface fluxes, atmospheric states
TFS/AFS	N	Y	Y	Y	Morning and afternoon	Y	Variances and covariances of CTP, HI_{low}, precipitation, surface fluxes
GLACE coupling strength (Ω)	Y	Y	Y	Y	Time means (~5 day)	N	Ensemble statistics from model simulations

[a] "Daytime" means (typically hourly) from sunrise through afternoon; data for some terms may be only for specific times or intervals.
[b] Can consider advection.

on systematic model biases in coupled processes that might otherwise have been overlooked in a classical model calibration–validation paradigm. Table 1 lists the metrics from Fig. 3 along with some of their characteristics, including the nature of input requirements (states versus fluxes and land versus atmosphere), spatial- and temporal-scale characteristics, and primary foundation for the metrics in terms of variables included. A selection of LoCo metrics and approaches, highlighted in Fig. 3, are described in more detail below.

Process-level metrics. MIXING DIAGRAMS AND THERMODYNAMICS. One diagnostic approach that incorporates components of the LoCo process chain is the concept of thermodynamic "mixing diagrams," demonstrated for LoCo applications by Santanello et al. (2009). This approach, first introduced by Stommel (1947), relates the daytime coevolution of 2-m potential temperature θ and humidity q to the full energy and water budgets and growth of the PBL. Mixing diagrams break down the evolution of θ and q into vector components that represent the flux contributions of surface heat (sensible) and moisture (latent) versus those from the atmosphere (including PBL entrainment and advection; see Betts 1992; Freedman and Fitzjarrald 2001). Mixing diagrams require only near-surface or mixed-layer temperature and humidity, surface fluxes, and PBL height information to infer entrainment fluxes that are notoriously difficult to observe (Lenschow and Stankov 1986; Grossman and Gamage 1995). Fortunately, to overcome the expense and difficulties of aircraft measurements, a new generation of ground-based active remote sensing systems permits the measurement of water vapor, temperature, and wind turbulence and flux profiles from the mixed to the entrainment layer (Muppa et al. 2016; Behrendt et al. 2015; Wulfmeyer et al. 2016; Bonin et al. 2017; Wulfmeyer et al. 2018).

Furthermore, the spread in model results due to different physics scheme combinations (e.g., LSM + PBL) can be evaluated directly against observations. Other well-known metrics like the Bowen ratio and lifting condensation level are inherent in this approach and can be used in complementary fashion to pinpoint weaknesses in the land and atmospheric components of coupled models (Santanello et al. 2009, 2011a,b, 2013a,b, 2015).

The coevolution of θ and q (as energy variables, J kg^{-1}) simulated by three different versions of a coupled mesoscale model [Advanced Research version of the Weather Research and Forecasting (WRF) Model (WRF-ARW) with Noah LSM] is shown for dry and wet soil moisture locations over the Southern Great Plains (SGP; Fig. 4; from Santanello et al. 2011a). Simulations were run with varying LSM–PBL combinations in WRF and allowed for the model to evolve in response to L-A interactions generated by each combination as compared with observations (using flux tower, radiosonde, and meteorological data). Overall, the results show that different soil moisture states lead to distinct diurnal patterns of θ and q evolution throughout the day. In this mixing diagram, vectors are defined for the daytime surface and atmospheric (advection + entrainment) flux contributions to the PBL budget. Over drier soils, significant warming and drying occurs due to strong surface heating (sensible heat flux) that leads to deep PBL growth and aggressive warm, dry air entrainment at the PBL top. Over wetter soils, there is strong surface moistening due to evaporation and little warming and drying throughout the day because of limited PBL growth and entrainment. Overall, these diagrams also demonstrate that, in order to further constrain the causes of model errors, it is desirable to have observing systems (such as that available at the SGP site shown here) that can measure a full suite of L-A variables including vertical profiles and sensible and latent heat and entrainment fluxes.

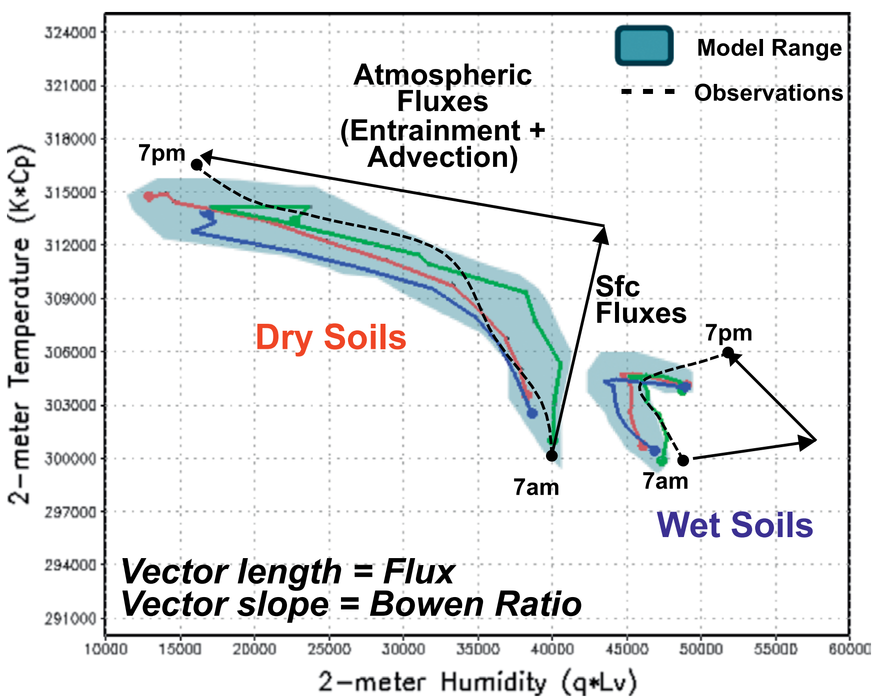

Fig. 4. Mixing diagrams showing coupling behavior of three different modeling schemes vs observations for dry and wet soil locations on 12 Jun 2002 over the SGP, as indicated by the diurnal (0700–1900 local time), hourly coevolution of 2-m temperature (*y* axis) and humidity (*x* axis) for a range of model simulations (green, red, and blue representing different PBL schemes in the WRF Model), observations (dashed black), and the derived surface and atmospheric flux vectors (black arrows). The *x* and *y* axes are in units of J kg^{-1} after multiplying humidity by the latent heat of vaporization and temperature by the specific heat, respectively. Adapted from Santanello et al. (2011a, their Fig. 1) based on experiments in Santanello et al. (2009).

CTP–HI$_{\text{LOW}}$. The convective triggering potential (CTP)–low-level humidity index (HI$_{\text{low}}$) framework [see Findell and Elthair (2003a,b) for details] was developed to better characterize the circumstances in which LoCo could influence afternoon convection, that is, when positive feedbacks (moist surface conditions increasing the chances of rain) or negative feedbacks (dry surface conditions increasing the chances of rain) were more likely to prevail or when large-scale atmospheric conditions would dictate the occurrence or absence of rain. It is built on the idea that early morning atmospheric profiles of temperature and humidity can provide information on whether boundary layer moistening or boundary layer deepening would be more likely to lead to convective triggering during the course of the day, or if the fluxes from the surface are unlikely to influence convective conditions. For example, if HI$_{\text{low}}$ indicates that the early morning lower atmosphere is extremely dry, moisture evaporated into the PBL from the surface cannot increase the PBL's moist static energy enough to allow for convection to occur. Such days are termed atmospherically controlled, as rain cannot be triggered by local surface processes (Fig. 5).

The CTP assesses the stability of the lower troposphere by measuring the departure of the temperature profile from moist adiabatic conditions in the region between 100 and 300 hPa above the ground surface. This is important because deep convection is triggered when the growing daytime PBL reaches the level of free convection (LFC). The lowering of the LFC during this period of boundary layer growth is impacted by the moist static energy within the boundary layer and the temperature lapse rate of the air through which the LFC falls: the LFC falls faster when the temperature profile is close to moist adiabatic. For convective triggering, high sensible heat flux accompanied by rapid PBL growth is more effective when the low-level atmospheric profile is near dry adiabatic and the CTP is high (a negative feedback), while PBL moistening accompanied by rapid LFC fall is a more effective mechanism when the lower atmosphere is close to moist adiabatic and CTP is low (a positive feedback). A negative CTP indicates the local atmosphere is too stable to convect; any rainfall would likely come from large-scale systems moving into the area during the course of the day.

Findell and Eltahir (2003b) used one-dimensional PBL modeling with U.S radiosonde data to map regions with frequent positive and negative feedback days (Fig. 5). Ferguson and Wood (2011) used satellite data sources to generate global maps of CTP, HI_{low}, and regional convective regime classifications of four types: local atmospheric conditions favoring convection over wet soils, over dry soils, and either supporting or suppressing convection, independent of land surface conditions. They developed a methodology to derive dataset-specific threshold values in CTP–HI_{low} parameter space that compensates both for biases in the satellite-derived datasets and for limitations of the original thresholds. Roundy et al. (2014) extended the work of Ferguson and Wood (2011) and developed the coupling drought index (CDI), which allows for day-to-day diagnosis of wet-soil advantage, dry-soil advantage, or atmospherically controlled conditions, given a long historical record to establish "climatological" joint probabilities between surface soil moisture, CTP, and HI_{low}. This allows for real-time assessment of convective sensitivity to local land surface conditions and has been used to better understand the role of the land surface in modulating drought events (Roundy et al. 2013, 2014; Roundy and Santanello 2017).

Heated condensation framework. The heated condensation framework (HCF; Tawfik and Dirmeyer 2014; Tawfik et al. 2015a,b) diagnoses the contribution of surface fluxes to convective initiation based on atmospheric profiles of temperature and humidity. The HCF differs from traditional convective diagnostic approaches; rather than lifting an isolated air parcel to quantify convective instability due to sensible heating and moisture flux, the HCF quantities are calculated by considering the well-mixed turbulent growth of the PBL. This construction emphasizes local buoyancy forced motions rather than large-scale mechanical parcel lifting and diagnoses a critical atmospheric level referred to as the buoyant condensation level (BCL). The BCL is the height where clouds would form atop a developing PBL through surface buoyancy fluxes alone. To find the BCL, the surface temperature is increased

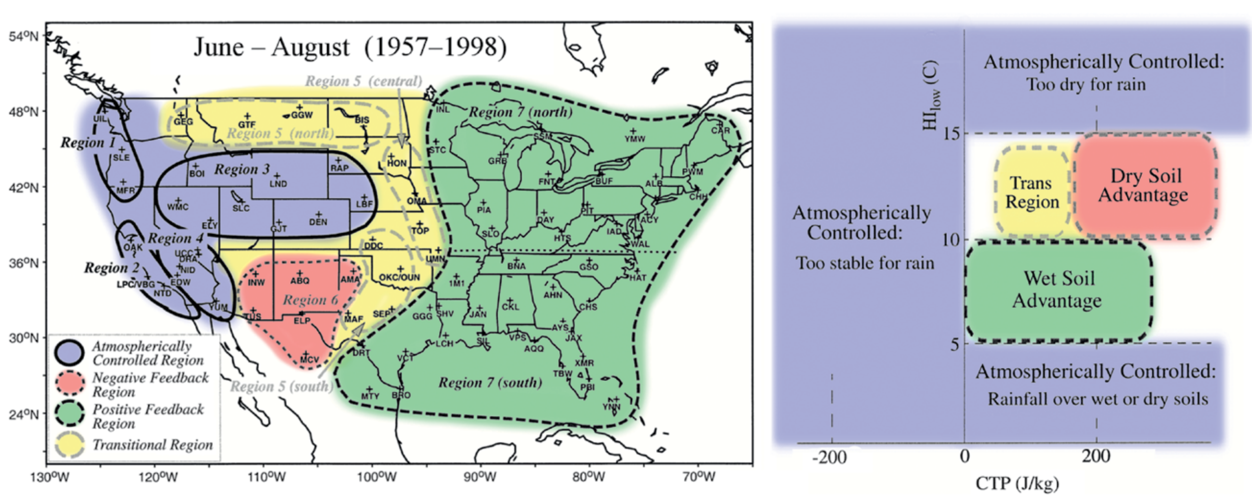

Fig. 5. (left) Regional categorizations based on the distribution of daily CTP–HI_{low} values at radiosonde stations (+) through the contiguous United States given (right) the CTP–HI_{low} framework (Findell and Eltahir 2003b).

incrementally, with the resulting heat mixed into the atmosphere producing an adiabatic temperature profile that intersects the original temperature profile at some height above the ground. The moisture within that depth is also mixed to a constant specific humidity. This incremental heating is repeated until saturation occurs at the top of the adiabatically mixed temperature profile, determining the BCL height. Locally triggered convection is initiated when no further surface heating is required (e.g., the PBL height equals the BCL height).

If some surface energy goes into evaporation instead of sensible heat flux, the PBL specific humidity would increase and the BCL would descend. However, that latent heat energy would be at the expense of sensible heat flux, and the lower BCL may not be reached as easily depending on the atmospheric profile. An optimum partitioning between sensible heat and moisture flux will trigger convection with the minimum total energy input. Surface soil moisture conditions and available energy (net surface radiation) may determine whether the PBL will grow to the BCL height. It should also be made clear that the HCF does not quantify the intensity of convection but rather whether convection is initiated locally.

Using the HCF, the atmospheric and land surface conditions leading up to any convective initiation can be quantified in models, reanalyses, or observations, elucidating emergent land–convection relationships. Figure 6 shows the percent chance of convective initiation given a morning convective inhibition (as defined by the HCF variable θ_{def}, which represents the temperature inputs needed in order for saturation to occur at the top of the mixed layer) and morning 10-cm soil moisture using 34 years of summer (June–August) reanalysis data from the North American Regional Reanalysis (NARR; Mesinger et al. 2006) over the contiguous United States, and indicates that these regions have between a 15% and 35% probability of local convective cloud initiation.

Starting from the regional average of soil moisture and θ_{def} over the southeastern United States (indicated by the SE in Fig. 6), the sensitivity of convective initiation to morning states of soil moisture and θ_{def} can be determined. For example, decreasing soil moisture from the 0.28 $m^3\ m^{-3}$ average to 0.15 $m^3\ m^{-3}$ would increase the likelihood of local convective initiation by roughly 10%. Overall, Fig. 6 shows that the likelihood of convective initiation is more sensitive to the morning state of θ_{def}, and soil moisture provides a secondary control on convective initiation. In addition to this emergent soil moisture–convective initiation relationship, the HCF also contains a set of other diagnostic quantities (not covered here) that quantify the most efficient surface energy partitioning needed to achieve convective initiation (Tawfik et al. 2015b).

Statistical metrics. SOIL MOISTURE MEMORY. As the first link of the process chain [Eq. (1)], soil moisture has the ability to influence the L-A processes over time and has been the focus of a number of quantitative metrics (e.g., Schlosser and Milly 2002; Betts 2004; Notaro 2008; Orlowsky and Seneviratne 2010; Mei and Wang 2012; Miralles et al. 2012; Roundy et al. 2013, 2014). Soil moisture memory (SMM) is a measure of the persistence of SM anomalies, which may then affect coupled feedbacks (e.g., McColl et al. 2017a,b). This is important because the soil accumulates and retains past precipitation and other weather anomalies (e.g., heat waves). This memory extends the impact of weather and climate events forward in time and can provide additional predictability of future weather and climate, improving predictions.

Delworth and Manabe (1988, 1989) showed that the time evolution of the surface water budget can be represented as a first-order Markov process, such that the lagged autocorrelation of soil moisture [defined as $r(\tau) = \exp(-\lambda\tau)$] has an *e*-folding time scale of $1/\lambda$ that can redden the spectrum of atmospheric

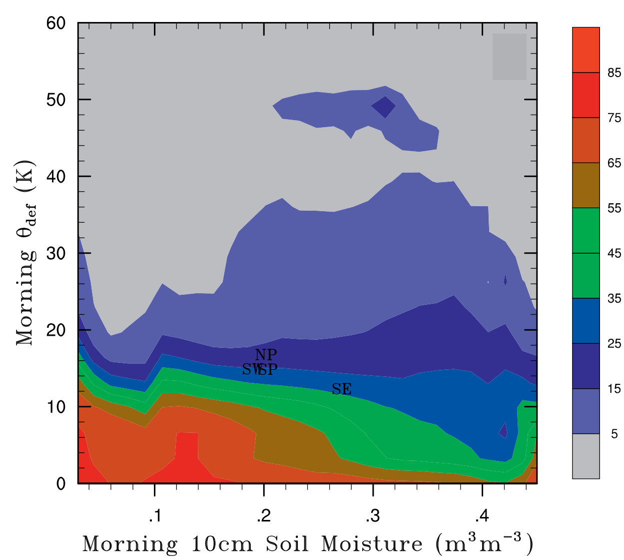

FIG. 6. Percent probability of triggering convection as a function of θ_{def} (a measure of convective inhibition) and 10-cm soil moisture derived from 34 years of daily NARR summer data. Average morning soil moisture and conditions are shown for four different regions over the United States: the Southeast (SE), the southern plains (SP), the northern plains (NP), and the Southwest (SW). Adapted from Tawfik et al. (2015a, their Fig. 11b).

variability where feedbacks are present. This time scale is typically defined as the SMM and is sensitive not only to the time spectrum of precipitation but also terrestrial hydrologic processes (e.g., infiltration, runoff, evapotranspiration), making it a tool to validate LSM simulation of these processes. SMM is generally calculated from long time series of data as a seasonally varying climatological characteristic of local hydrology (cf. Koster and Suarez 2001). SMM has been estimated in observational studies (e.g., Vinnikov and Yeserkepova 1991; Koster et al. 2003; Dirmeyer et al. 2016) and applied as a robust metric for verifying soil moisture persistence in both uncoupled and coupled LSMs and across observational datasets from in situ to satellite instruments (e.g., Robock et al. 1995; Koster and Suarez 2001; Seneviratne and Koster 2012; Dirmeyer et al. 2013; Hagemann and Stacke 2015). It should be noted that the frequency of data (observations or model output) affects the estimation, so care must be taken when comparing results; longer periods between samples (weekly instead of daily, or monthly instead of weekly) act as a low-pass time filter, removing higher frequencies from consideration.

Two-legged metrics. The most common multivariate statistic is the correlation $r(v_1, v_2)$, where high correlations between variables can hint at causality. However, high correlations within the LoCo process chain do not guarantee important feedbacks are acting. For instance, in the Sahara there are very strong correlations between soil moisture and evapotranspiration (ET), but there is rarely enough soil moisture to contribute to meaningful evaporation. To have an impact on the atmosphere, there must be sufficient variability in the terms over time. Guo et al. (2006) recognized this and presented a metric combining correlation and standard deviation σ. Dirmeyer (2011b) generalized this as a terrestrial coupling index I, noting the relationship

$$I = \sigma_\phi r(\mathrm{SM}, \phi) = \sigma_{\mathrm{SM}} \frac{d\phi}{d\mathrm{SM}}, \tag{2}$$

where the linear regression slope of surface flux ϕ on SM, $d\phi/d\mathrm{SM}$, is a measure of the sensitivity of ϕ to SM. Like CTP–$\mathrm{HI}_{\mathrm{low}}$, coupling indices are calculated from large time series of daily (or longer) data.

Progressing along the process chain in Eq. (1) to the response of atmospheric states to surface fluxes, coupling indices for the atmospheric leg can also be generated using the same formulation in Eq. (2), but substituting the surface fluxes for soil moisture and atmospheric properties for the surface fluxes. When atmospheric leg indices are paired with indices from the terrestrial leg, we have "two legged" coupling metrics showing the potential link from land surface states to atmospheric responses. Separate pathways in the process chain through the heat and moisture cycles can be examined, for example, noting the strong relationships between surface sensible heat flux and daytime PBL growth (Betts 2004).

Two-legged metrics are easily applied to model output, provided that the necessary variables are saved and complete in time and space. Figure 7 shows the global distribution of terrestrial (through the moisture variables, SM, and latent heat flux) and atmospheric (through the thermal variables, sensible heat flux, and PBL height) legs for boreal and austral summers estimated from multidecade simulations of the operational coupled L-A model from the European Centre for Medium-Range Weather Forecasts (ECMWF; Dirmeyer et al. 2012). Application to observed data can be more challenging as surface flux measurements are not widespread or typically long term. For the terrestrial leg, collocated soil moisture, and surface flux measurements are necessary. For the atmospheric leg, collocated surface flux and meteorological or profile measurements are necessary. There is also a seasonality in coupling that is made evident using these metrics, as seen in Fig. 7.

Triggering and amplification feedback strength. Findell et al. (2011) evaluated the sensitivity of afternoon rainfall to morning EF using 25 years of data from the North American Regional Reanalysis dataset (NARR; Mesinger et al. 2006). The EF dependence on rainfall was assessed using two statistical metrics: triggering feedback strength (TFS), which reflects how afternoon rainfall frequency changes with EF, and amplification feedback strength (AFS), which quantifies how accumulated rainfall varies with EF on those afternoons when rainfall occurs. They are defined as

$$\mathrm{TFS} = \sigma_{\mathrm{EF}} \frac{\partial \Gamma(r)}{\partial \mathrm{EF}}; \ \mathrm{AFS} = \sigma_{\mathrm{EF}} \frac{\partial E[r]}{\partial \mathrm{EF}}, \tag{3}$$

where σ_{EF} is the standard deviation of evaporative fraction, $\Gamma(r)$ is the probability of afternoon rainfall occurrence, and $E[r]$ is the expected value of rainfall amount when rainfall does occur (>1 mm).

To limit the analysis to local conditions when large-scale forcing was not dominant, TFS was calculated using data from only summertime days with no rain in the morning and with CTP > 0. Days contributing to the AFS calculation were further limited to those when afternoon rainfall occurred. This work showed that high evaporation enhances

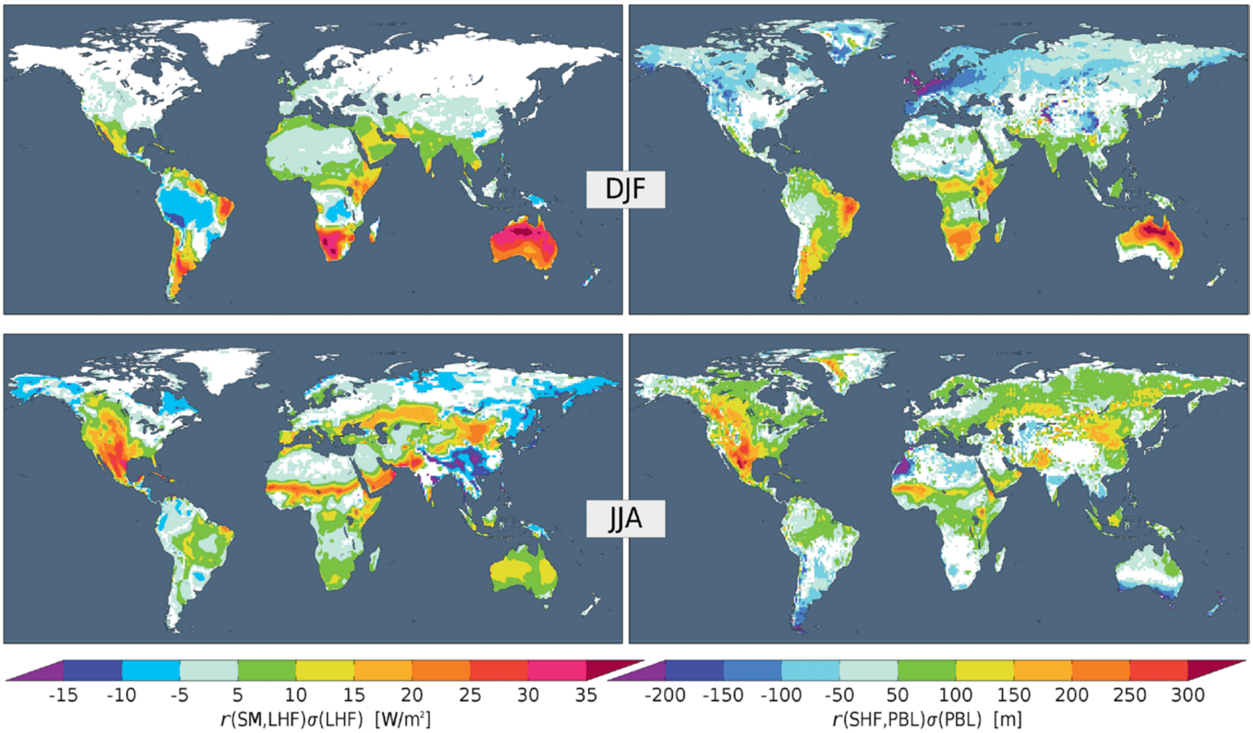

Fig. 7. (left) Terrestrial and (right) atmospheric coupling indices based on the formulation in Eq. (2) for the indicated seasons: SM is soil moisture, LHF is latent heat flux, SHF is sensible heat flux, and PBL is height of the planetary boundary layer. Positive values indicate coupling, and insignificant correlations are masked. Adapted from Dirmeyer et al. (2012, their Fig. 8).

the probability of afternoon rainfall over the United States, primarily east of the Mississippi River (Fig. 8). Variations in surface fluxes were shown to lead to 10%–25% changes in afternoon rainfall probability in these regions (Fig. 8a). The intensity of rainfall, by contrast, was largely insensitive to surface fluxes (Fig. 8b). These results indicate that while surface flux partitioning can shift the local atmosphere from non-convecting to convecting in non-moisture-limited regions, other controls such as free-tropospheric moisture content or large-scale moisture convergence largely determine how much rainfall occurs.

Findell et al. (2011) suggest that local surface fluxes represent an important trigger for convective rainfall in the eastern United States during the summer, leading to a positive evaporation–precipitation feedback. This focus on the impact of surface fluxes on subsequent rainfall does not include the soil moisture portion of the process chain in Fig. 2 (arrow a), but is a statistical assessment of the net sensitivity of ΔP to ΔEF (arrows b–d). Berg et al. (2013) showed results from a GCM with similar TFS and AFS signatures as the NARR model data, but demonstrated that the GCM's TFS resulted from a weaker sensitivity of rainfall to EF than the NARR model data yet showed enhanced variability of EF, highlighting the complexity of characterization of interdependent processes. In addition, Guillod et al. (2014) showed that the TFS patterns are sensitive to the choice of observational data, highlighting the need for better constrained observations of surface turbulent fluxes.

RESOURCES AND OUTREACH.

In addition to the GEWEX, GLASS, and LoCo websites (www.gewex.org/loco/), there have been a number of resources developed by the LoCo Working Group to help support community involvement.

The Coupling Metrics Toolkit. The Coupling Metrics Toolkit (CoMeT; www.coupling-metrics.com) is an open-source code package for calculating selected LoCo coupling metrics. Specifically, CoMeT is a set of portable FORTRAN 90 modules with thorough inline documentation currently available via a Git repository. The modules are designed to be easily wrapped into existing Python or NCAR Common Language (NCL) code using the *f2py* and *WRAPIT* commands, respectively. Development of CoMeT was motivated by the growing need from the broader research community to examine L-A coupling and interactions and the lack of a standard code package to facilitate calculation. Currently CoMeT contains

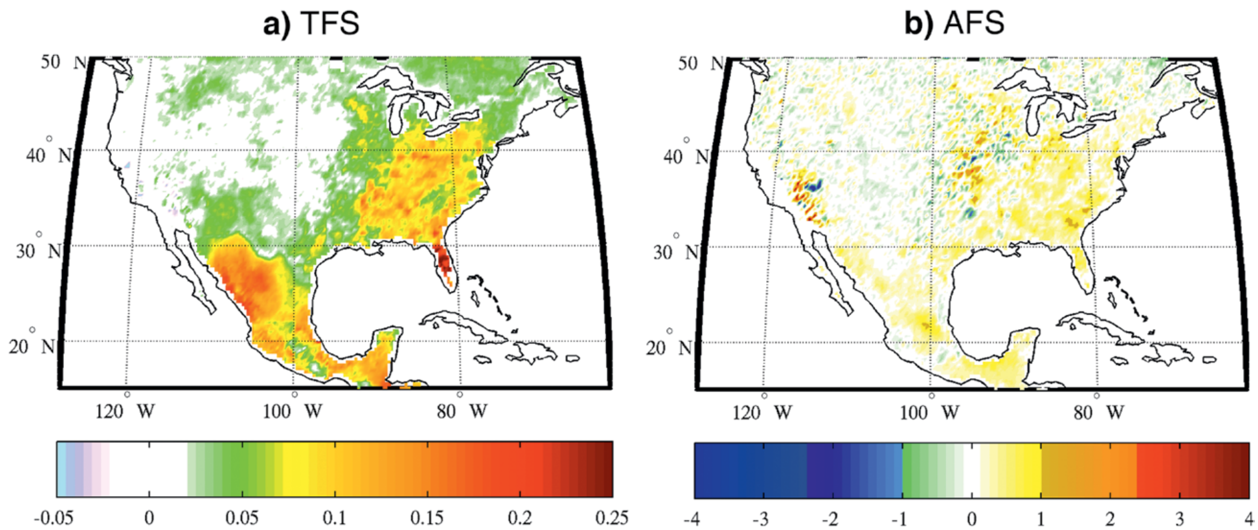

Fig. 8. The sensitivity of convective triggering and rainfall amount to evaporative fraction. (a) TFS [units of probability of afternoon (1200–1800 local time) rain] and (b) AFS (units of millimeters of afternoon rain) during Jun–Aug, derived from 25 years of NARR data (Findell et al. 2011).

six metrics, five of which are discussed in this article: 1) SMM, 2) the variables from the mixing diagram approach, 3) CTP–HI_{low}, 4) the two-legged coupling indices, 5) HCF, and 6) the relative humidity (RH) tendency (Ek and Mahrt 1994; Ek and Holtslag 2004; Gentine et al. 2013b). Future plans for CoMeT include a Python-based wrapper that would allow users to specify the path to data and desired metrics, where CoMeT would return an output file with the results. This will enable a friendlier interface that does not require the user to write wrapping code. Because this resource is intended for broad use, community input and requests regarding additional metrics are highly welcome.

Quick reference for metrics. A growing reference catalog of L-A coupling metrics is maintained at http://cola.gmu.edu/dirmeyer/Coupling_metrics.html. Some two dozen metrics are listed, with links to single-page PDF documents on each that give a basic description, input/variable requirements, applicability, caveats, and references for further information. The catalog also outlines to which portion of the LoCo process chain each metric is relevant, the applicable space and time scales of the metric, and whether it can be estimated from observational data (cf. Table 1 for a subset). As with CoMeT, this is a community resource that can expand to accommodate new metrics, and user input is welcome.

Community connections. LoCo Working Group members serve to facilitate and advocate for L-A coupling considerations in several science communities. As with the LoCo metrics, these connections span a wide range of scales and applications and aim to increase awareness of the role of L-A interactions in weather and climate. This includes the subseasonal-to-seasonal (S2S) prediction community (Vitart et al. 2017), where LoCo has been utilized to elucidate how global models should initialize their LSMs. This also includes strong involvement in the planning and execution of field campaigns and dataset production like those led by the U.S. Department of Energy's Atmospheric Radiation Measurement (ARM) program's SGP test bed. Over the past 20 years, the ARM community has utilized observations of the PBL to investigate L-A interactions from a mostly atmospheric perspective (e.g., Berg and Stull 2004; Zhang and Klein 2010), and the SGP site has recently undergone significant reconfiguration to better monitor L-A interactions, including new soil moisture sensors and an overall instrument synergy that spans the LoCo process chain. LoCo efforts have helped lead to development of "best estimate" products of land surface [ARM Best Estimate (ARMBE)-Land; Xie et al. 2010] and additional PBL profile measurements [Enhanced Soundings for Local Coupling Studies Field Campaign (ESLCS; Ferguson et al. 2016)] complementing the traditional suite of atmospheric measurements to more fully assess coupled processes and utilize LoCo metrics. Ongoing and future campaigns over the SGP are focused on the surface layer (<100 m above surface; Cheng et al. 2017). L-A interactions, including the observation and theoretical derivation of key variables in the PBL such as variance and flux profiles as well as entrainment fluxes, have recently become available, for example, within the LAFE (Wulfmeyer and Turner 2016; Wulfmeyer et al. 2018), which can be applied for testing new similarity relationships (Wulfmeyer et al. 2016) and extended analyses of LoCo metrics.

LoCo is supporting the organization of a North American regional hydroclimate project (www.gewex.org/panels/gewex-hydroclimatology-panel/regional-hydroclimate-projects-rhps/north-american-regional-hydroclimate-project-initiative/) under GEWEX's water availability grand challenge, and it convenes or contributes to numerous conference sessions, workshops, and yearly summer schools. LoCo also contributes to the National Research Council Decadal Survey by identifying gaps in our observational suite, especially from space, that are needed to utilize LoCo metrics to further improve understanding of L-A coupling.

CHALLENGES AND THE FUTURE OF LOCO. It is evident that the scope of LoCo, defined by Eq. (1), captures only a subset of L-A processes and types of coupling that exist in nature. However, the LoCo paradigm serves as a foundation, rooted in water and energy exchanges, from which to expand upon in terms of breadth and complexity. As the second decade of LoCo begins, the Working Group has broadened its scope to consider cold processes (snow, ice), radiation and cloud feedbacks, spatial SM–*P* feedbacks, human land and water management impacts (drainage, irrigation, land-use/land-cover change, dams), soils and groundwater, biogeochemistry (carbon), vegetation state (e.g., Williams and Torn 2015), and stress (solar-induced fluorescence, transpiration) and to extend to phenomena such as monsoons and landfalling tropical cyclones. There is also a strong push to extend to nighttime/stable coupling assessment and interactions with the PBL community. The expanding themes are reflective of science steering at higher levels within GEWEX and WCRP, as well as new areas of expertise represented within the LoCo Working Group. There is also work to quantify the relative contribution of local versus external forcing to event- and seasonal-scale L-A coupling strength, in the midst of internal variability (e.g., Song et al. 2016; Ford et al. 2015; Berg et al. 2017a,b). This evolution coincides with, and contributes to, the evolution of Earth system models that encapsulate additional processes, but at the same time require more complex and quantitative metrics to employ in their development.

In terms of recent community-based projects, there are direct connections that are being made to the GEWEX Diurnal Land/Atmosphere Coupling Experiment (DICE; http://appconv.metoffice.com/dice/dice.html) and the Protocol for the Analysis of Land Surface Models (PALS) Land Surface Model Benchmarking Evaluation Project (PLUMBER; Best et al. 2015; Haughton et al. 2016); the latter can provide a paradigm for extending model benchmarking vertically into the atmosphere. LoCo is also connected to the GLACE modeling community via the GLACE-CMIP5 project (Seneviratne et al. 2013), which seeks to evaluate SM–atmosphere coupling and its impact on climate change in models using idealized GCM simulations with and without interactive SM (e.g., Berg et al. 2016, 2017a,b), and LoCo approaches have been used to find coherency in trends as part of the Intergovernmental Panel on Climate Change Fifth Assessment Report (van Heerwaarden et al. 2010). Likewise, as the CMIP6 exercise comes to fruition, LoCo will look to support and inform the analysis of climate model simulations, in particular modeling experiments focusing on the role of land surface processes, such as soil moisture and snow feedbacks [Land Surface, Snow and Soil Moisture Model Intercomparison Project (LS3MIP); van den Hurk et al. 2016].

The theme of the 2017 American Meteorological Society Annual Meeting—"Observations Lead the Way"—is also highly relevant to the success of LoCo. Advanced metrics are only as good as the observations applied to confront models. While tremendous progress has been made in retrieving components of the water cycle (e.g., soil moisture, clouds, precipitation) from space, the layer of interaction between the land and atmosphere (i.e., the PBL and its diurnal evolution) remains largely undersampled, and thus the full suite of variables needed to assess the process chain in Eq. (1) has been very difficult to observe completely at the necessary spatial or temporal scales (Findell et al. 2015). It is also clear that the metrics most useful in terms of characterizing L-A feedback include variables that contain the characteristics of the PBL from which entrainment fluxes and atmospheric boundary layer depth are most important and can also be observed. In particular, the lack of continuous monitoring of the lower troposphere (the PBL "gap") has become quite evident. Therefore, the community must also support 1) the development and application of suitable observing systems to address L-A coupling and 2) the design and the application of a suitable sensor synergy to directly measure the required components of coupling metrics without any use of model data.

To this end, there is now increasing activity in ground-based PBL profiling using active remote sensing techniques that will likely lead to methods that can be applied to future satellite missions (Wulfmeyer et al. 2015). Efforts to produce long- (Liu et al. 2012), medium- (Kolassa et al. 2016, 2017), and short-term (R. Bindlish 2017, personal communication) homogenized satellite-based soil moisture records, a surface flux record [e.g., Water, Energy, and Carbon with Artificial Neural Networks (WECANN; Alemohammad et al. 2017)], and within-GEWEX subdaily precipitation records (e.g., Blenkinsop et al. 2017) will further enable observationally based LoCo studies in the future.

Finally, the ultimate utility of improved understanding of the physical processes driving the L-A system should be felt in advancing our community models, improving weather and climate predictions, and ultimately enhancing decision-making capabilities that protect life and property. This will require a change in model development philosophy, where parameterizations in GCMs and LSMs are not developed in separation but as linked parts of a coupled system that are calibrated, validated, and diagnosed together. Closer connections between research and operational communities, including joint development of benchmarks for coupled L-A modeling, will greatly aid progress, and we invite interested readers to contact the authors and/or refer to the LoCo website for more information. These are the ultimate aims of the LoCo community—building effective scientific linkages that mirror the links we are recognizing in nature.

ACKNOWLEDGMENTS. The authors thank GEWEX and the GLASS panel for their moral and programmatic support, LoCo working group members (past and present), and specifically the pioneers in L-A research that supported the LoCo idea from the beginning, including Alan Betts, Christa Peters-Lidard, Bart van den Hurk, Martin Best, and Paul Houser. We would also like to thank the DOE-ARM program for welcoming the land/LoCo community into their strategic planning. This work was supported by NASA Grants 15-SUSMAP15-0147 and 12-MAP12-0045.

REFERENCES

Alemohammad, S. H., and Coauthors, 2017: Water, Energy, and Carbon with Artificial Neural Networks (WECANN): A statistically based estimate of global surface turbulent fluxes and gross primary productivity using solar-induced fluorescence. *Biogeosciences*, **14**, 4101–4124, https://doi.org/10.5194/bg-14-4101-2017.

Andersen, T., and J. M. Shepherd, 2014: A global spatiotemporal analysis of inland tropical cyclone maintenance or intensification. *Int. J. Climatol.*, **34**, 391–402, https://doi.org/10.1002/joc.3693.

Anderson, B. T., A. C. Ruane, J. O. Roads, and M. Kanamitsu, 2009: Estimating the influence of evaporation and moisture-flux convergence upon seasonal precipitation rates. Part II: An analysis for North America based upon the NCEP-DOE Reanalysis II Model. *J. Hydrometeor.*, **10**, 893–911, https://doi.org/10.1175/2009JHM1063.1.

Behrendt, A., V. Wulfmeyer, E. Hammann, S. K. Muppa, and S. Pal, 2015: Profiles of second- to third-order moments of turbulent temperature fluctuations in the convective boundary layer: First measurements with rotational Raman lidar. *Atmos. Chem. Phys.*, **15**, 5485–5500, https://doi.org/10.5194/acp-15-5485-2015.

Berg, A., K. Findell, B.R. Lintner, P. Gentine, and C. Kerr, 2013: Precipitation sensitivity to surface heat fluxes over North America in reanalysis and model data. *J. Hydrometeor.*, **14**, 722–743, https://doi.org/10.1175/JHM-D-12-0111.1.

——, and Coauthors, 2016: Land–atmosphere feedbacks amplify aridity increase over land under global warming. *Nat. Climate Change*, **6**, 869–874, https://doi.org/10.1038/nclimate3029.

——, B. Lintner, K. Findell, and A. Giannini, 2017a: Soil moisture influence on seasonality and large-scale circulation in simulations of the West African monsoon. *J. Climate*, **30**, 2295–2317, https://doi.org/10.1175/JCLI-D-15-0877.1.

——, ——, ——, and ——, 2017b: Uncertain soil moisture feedbacks in model projections of Sahel precipitation. *Geophys. Res. Lett.*, **44**, 6124–6133, https://doi.org/10.1002/2017GL073851.

Berg, L. K., and R. B. Stull, 2004: Parameterization of joint frequency distributions of potential temperature and water vapor mixing ratio in the daytime convective boundary layer. *J. Atmos. Sci.*, **61**, 813–828, https://doi.org/10.1175/1520-0469(2004)061<0813:POJFDO>2.0.CO;2.

Best, M. J., and Coauthors, 2015: The plumbing of land surface models: Benchmarking model performance. *J. Hydrometeor.*, **16**, 1425–1442, https://doi.org/10.1175/JHM-D-14-0158.1.

Betts, A. K., 1992: FIFE atmospheric boundary layer budget methods. *J. Geophys. Res.*, **97**, 18 523–18 531, https://doi.org/10.1029/91JD03172.

——, 2000: Idealized model for equilibrium boundary layer over land. *J. Hydrometeor.*, **1**, 507–523, https://doi.org/10.1175/1525-7541(2000)001<0507:IMFEBL>2.0.CO;2.

——, 2004: Understanding hydrometeorology using global models. *Bull. Amer. Meteor. Soc.*, **85**, 1673–1688, https://doi.org/10.1175/BAMS-85-11-1673.

——, and P. Viterbo, 2005: Land-surface, boundary layer, and cloud-field coupling over the southwestern

Amazon in ERA-40. *J. Geophys. Res.*, **110**, D14108, https://doi.org/10.1029/2004JD005702.
——, and M. A. F. Silva Dias, 2010: Progress in understanding land-surface-atmosphere coupling from LBA research. *J. Adv. Model. Earth Syst.*, **2**, 6, https://doi.org/10.3894/JAMES.2010.2.6.
——, A. G. Barr, A. C. M. Beljaars, M. J. Miller, and P. A. Viterbo, 1996: The land surface-atmosphere interaction: A review based on observational and global modeling perspectives. *J. Geophys. Res.*, **101**, 7209–7225, https://doi.org/10.1029/95JD02135.
——, A. B. Tawfik, and R. L. Desjardins, 2017: Revisiting hydrometeorology using cloud and climate observations. *J. Hydrometeor.*, **18**, 939–955, https://doi.org/10.1175/JHM-D-16-0203.1.
Blenkinsop, S., E. Lewis, S. C. Chan, and H. J. Fowler, 2017: Quality-control of an hourly rainfall dataset and climatology of extremes for the UK. *Int. J. Climatol.*, **37**, 722–740, https://doi.org/10.1002/joc.4735.
Bonin, T. A., and Coauthors, 2017: Evaluation of turbulence measurement techniques from a single Doppler lidar. *Atmos. Meas. Tech.*, **10**, 3021–3039, https://doi.org/10.5194/amt-10-3021-2017.
Brubaker, K. L., and D. Entekhabi, 1996: Asymmetric recovery from wet versus dry soil moisture anomalies. *J. Appl. Meteor.*, **35**, 94–109, https://doi.org/10.1175/1520-0450(1996)035<0094:ARFWVD>2.0.CO;2.
Cheng, Y., C. Sayde, Q. Li, J. Basara, J. Selker, E. Tanner, and P. Gentine, 2017: Failure of Taylor's hypothesis in the atmospheric surface layer and its correction for eddy-covariance measurements. *Geophys. Res. Lett.*, **44**, 4287–4295, https://doi.org/10.1002/2017GL073499.
Delworth, T. L., and S. Manabe, 1988: The influence of potential evaporation on the variabilities of simulated soil wetness and climate. *J. Climate*, **1**, 523–547, https://doi.org/10.1175/1520-0442(1988)001<0523:TIOPEO>2.0.CO;2.
——, and ——, 1989: The influence of soil wetness on near-surface atmospheric variability. *J. Climate*, **2**, 1447–1462, https://doi.org/10.1175/1520-0442(1989)002<1447:TIOSWO>2.0.CO;2.
de Noblet-Ducoudré, N., and Coauthors, 2012: Determining robust impacts of land-use-induced land cover changes on surface climate over North America and Eurasia: Results from the first set of LUCID experiments. *J. Climate*, **25**, 3261–3281, https://doi.org/10.1175/JCLI-D-11-00338.1.
Diak, G. R., 1990: Evaluation of heat flux, moisture flux and aerodynamic roughness at the land surface from knowledge of the PBL height and satellite derived skin temperatures. *Agric. For. Meteor.*, **52**, 181–198, https://doi.org/10.1016/0168-1923(90)90105-F.
Dirmeyer, P. A., 2011a: A history of the Global Soil Wetness Project (GSWP). *J. Hydrometeor.*, **12**, 729–749, https://doi.org/10.1175/JHM-D-10-05010.1.
——, 2011b: The terrestrial segment of soil moisture–climate coupling. *Geophys. Res. Lett.*, **38**, L16702, https://doi.org/10.1029/2011GL048268.
——, and S. Halder, 2016: Sensitivity of numerical weather forecasts to initial soil moisture variations in CFSv2. *Wea. Forecasting*, **31**, 1973–1983, https://doi.org/10.1175/WAF-D-16-0049.1.
——, R. D. Koster, and Z. Guo, 2006: Do global models properly represent the feedback between land and atmosphere? *J. Hydrometeor.*, **7**, 1177–1198, https://doi.org/10.1175/JHM532.1.
——, C. A. Schlosser, and K. L. Brubaker, 2009: Precipitation, recycling, and land memory: An integrated analysis. *J. Hydrometeor.*, **10**, 278–288, https://doi.org/10.1175/2008JHM1016.1.
——, and Coauthors, 2012: Evidence for enhanced land–atmosphere feedback in a warming climate. *J. Hydrometeor.*, **13**, 981–995, https://doi.org/10.1175/JHM-D-11-0104.1.
——, S. Kumar, M. J. Fennessy, E. L. Altshuler, T. DelSole, Z. Guo, B. Cash, and D. Straus, 2013: Model estimates of land-driven predictability in a changing climate from CCSM4. *J. Climate*, **26**, 8495–8512, https://doi.org/10.1175/JCLI-D-13-00029.1.
——, and Coauthors, 2016: Confronting weather and climate models with observational data from soil moisture networks over the United States. *J. Hydrometeor.*, **17**, 1049–1067, https://doi.org/10.1175/JHM-D-15-0196.1.
Dolman, A., J. Gash, J. Goutorbé, Y. Kerr, T. Lebel, S. Prince, and J. Stricker, 1997: The role of the land surface in Sahelian climate: HAPEX–Sahel results and future research needs. *J. Hydrol.*, **188–189**, 1067–1079, https://doi.org/10.1016/S0022-1694(96)03183-6.
Ek, M. B., and L. Mahrt, 1994: Daytime evolution of relative humidity at the boundary-layer top. *Mon. Wea. Rev.*, **122**, 2709–2721, https://doi.org/10.1175/1520-0493(1994)122<2709:DEORHA>2.0.CO;2.
——, and A. A. M. Holtslag, 2004: Influence of soil moisture on boundary layer cloud development. *J. Hydrometeor.*, **5**, 86–99, https://doi.org/10.1175/1525-7541(2004)005<0086:IOSMOB>2.0.CO;2.
Ferguson, C. R., and E. F. Wood, 2011: Observed land–atmosphere coupling from satellite remote sensing and reanalysis. *J. Hydrometeor.*, **12**, 1221–1254, https://doi.org/10.1175/2011JHM1380.1.
——, ——, and R. K. Vinukollu, 2012: A global intercomparison of modeled and observed land–atmosphere coupling. *J. Hydrometeor.*, **13**, 749–784, https://doi.org/10.1175/JHM-D-11-0119.1.

——, J. Santanello, and P. Gentine, 2016: Enhanced soundings for local coupling studies field campaign report. Rep. DOE/SC-ARM-16-023, 30 pp., www.arm.gov/publications/programdocs/doe-sc-arm-16-023.pdf.

Findell, K. L., and E. A. B. Eltahir, 2003a: Atmospheric controls on soil moisture–boundary layer interactions: Part I: Framework development. *J. Hydrometeor.*, **4**, 552–569, https://doi.org/10.1175/1525-7541(2003)004<0552:ACOSML>2.0.CO;2.

——, and ——, 2003b: Atmospheric controls on soil moisture–boundary layer interactions: Part II: Feedbacks within the continental United States. *J. Hydrometeor.*, **4**, 570–583, https://doi.org/10.1175/1525-7541(2003)004<0570:ACOSML>2.0.CO;2.

——, E. Shevliakova, P. C. Milly, and R. J. Stouffer, 2007: Modeled impact of anthropogenic land cover change on climate. *J. Climate*, **20**, 3621–3634, https://doi.org/10.1175/JCLI4185.1.

——, P. Gentine, B. R. Linter, and C. Kerr, 2011: Probability of afternoon precipitation in eastern United States and Mexico enhanced by high evaporation. *Nat. Geosci.*, **4**, 434–439, https://doi.org/10.1038/ngeo1174.

——, ——, ——, and B. P. Guillod, 2015: Data length requirements for observational estimates of land–atmosphere coupling strength. *J. Hydrometeor.*, **16**, 1615–1635, https://doi.org/10.1175/JHM-D-14-0131.1.

——, A. Berg, P. Gentine, J. P. Krasting, B. R. Lintner, S. Malyshev, J. A. Santanello Jr., and E. Shevliakova, 2017: The impact of anthropogenic land use and land cover change on regional climate extremes. *Nat. Commun.*, **8**, 989, https://doi.org/10.1038/s41467-017-01038-w.

Ford, T. W., A. D. Rapp, and S. M. Quiring, 2015: Does afternoon precipitation occur preferentially over dry or wet soils in Oklahoma? *J. Hydrometeor.*, **16**, 874–888, https://doi.org/10.1175/JHM-D-14-0005.1.

Freedman, J. M., and D. R. Fitzjarrald, 2001: Postfrontal airmass modification. *J. Hydrometeor.*, **2**, 419–437, https://doi.org/10.1175/1525-7541(2001)002<0419:PAM>2.0.CO;2.

Gentine, P., A. A. M. Holtslag, F. D'Andrea, and M. Ek, 2013a: Surface and atmospheric controls on the onset of moist convection over land. *J. Hydrometeor.*, **14**, 1443–1461, https://doi.org/10.1175/JHM-D-12-0137.1.

——, C. R. Ferguson, and A. A. M. Holtslag, 2013b: Diagnosing evaporative fraction over land from boundary-layer clouds. *J. Geophys. Res. Atmos.*, **118**, 8185–8196, https://doi.org/10.1002/jgrd.50416.

Green, J. K., A. G. Konings, S. H. Alemohammad, J. Berry, D. Entekhabi, J. Kolassa, J.-E. Lee, and P. Gentine, 2017: Regionally strong feedbacks between the atmosphere and terrestrial biosphere. *Nat. Geosci.*, **10**, 410–414, https://doi.org/10.1038/ngeo2957.

Grossman, R. L., and N. Gamage, 1995: Moisture flux and mixing processes in the daytime continental convective boundary layer. *J. Geophys. Res.*, **100**, 25 665–25 674, https://doi.org/10.1029/95JD00853.

Guillod, B. P., and Coauthors, 2014: Land-surface controls on afternoon precipitation diagnosed from observational data: Uncertainties and confounding factors. *Atmos. Chem. Phys.*, **14**, 8343–8367, https://doi.org/10.5194/acp-14-8343-2014.

——, B. Orlowsky, D. G. Miralles, A. J. Teuling, and S. I. Seneviratne, 2015: Reconciling spatial and temporal soil moisture effects on afternoon rainfall. *Nat. Commun.*, **6**, 6443, https://doi.org/10.1038/ncomms7443.

Guo, Z., and Coauthors, 2006: GLACE: The Global Land–Atmosphere Coupling Experiment. Part II: Analysis. *J. Hydrometeor.*, **7**, 611–625, https://doi.org/10.1175/JHM511.1.

Hagemann, S., and T. Stacke, 2015: Impact of the soil hydrology scheme on simulated soil moisture memory. *Climate Dyn.*, **44**, 1731–1750, https://doi.org/10.1007/s00382-014-2221-6.

Hall, F. G., and P. J. Sellers, 1995: First International Satellite Land Surface Climatology Project (ISLSCP) Field Experiment (FIFE) in 1995. *J. Geophys. Res.*, **100**, 25 383–25 396, https://doi.org/10.1029/95JD03300.

Haughton, N., and Coauthors, 2016: The plumbing of land surface models: Why are models performing so poorly? *J. Hydrometeor.*, **17**, 1705–1723, https://doi.org/ 10:1075/JHM-D-15-0171.1.

Henderson-Sellers, A., Z.-L. Yang, and R. E. Dickinson, 1993: The Project for Intercomparison of Land-surface Parameterization Schemes. *Bull. Amer. Meteor. Soc.*, **74**, 1335–1349, https://doi.org/10.1175/1520-0477(1993)074<1335:TPFIOL>2.0.CO;2.

——, A. J. Pitman, P. Irannejad, and K. McGuffie, 2002: Land surface simulations improve atmospheric modeling. *Eos, Trans. Amer. Geophys. Union*, **83**, 145–152, https://doi.org/10.1029/2002EO000091.

Hirsch, A. L., J. Kala, A. J. Pitman, C. Carouge, J. P. Evans, V. Haverd, and D. Mocko, 2014: Impact of land surface initialization approach on subseasonal forecast skill: A regional analysis in the Southern Hemisphere. *J. Hydrometeor.*, **15**, 300–319, https://doi.org/10.1175/JHM-D-13-05.1.

——, A. J. Pitman, J. Kala, R. Lorenz, and M. G. Donat, 2015: Modulation of land-use change impacts on temperature extremes via land–atmosphere coupling over Australia. *Earth Interact.*, **19**, https://doi.org/10.1175/EI-D-15-0011.1.

Hsu, H., M.-H. Lo, B. P. Guillod, D. G. Miralles, and S. Kumar, 2017: Relation between precipitation location and antecedent/subsequent soil moisture spatial patterns. *J. Geophys. Res. Atmos.*, **122**, 6319–6328, https://doi.org/10.1002/2016JD026042.

Jimenez, P. A., J. V. de Arellano, J. Navarro, and J. F. Gonzalez-Rouco, 2014: Understanding land–atmosphere interactions across a range of spatial and temporal scales. *Bull. Amer. Meteor. Soc.*, **95**, ES14–ES17, https://doi.org/10.1175/BAMS-D-13-00029.1.

Kleidon, A., and M. Heimann, 1998: Optimised rooting depth and its impacts on the simulated climate of an atmospheric general circulation model. *Geophys. Res. Lett.*, **25**, 345–348, https://doi.org/10.1029/98GL00034.

Knist, S., and Coauthors, 2017: Land-atmosphere coupling in EURO-CORDEX evaluation experiments. *J. Geophys. Res. Atmos.*, **122**, 79–103, https://doi.org/10.1002/2016JD025476.

Kolassa, J., P. Gentine, C. Prigent, and F. Aires, 2016: Soil moisture retrieval from AMSR-E and ASCAT microwave observation synergy. Part 1: Satellite data analysis. *Remote Sens. Environ.*, **173**, 1–14, https://doi.org/10.1016/j.rse.2015.11.011.

——, ——, ——, ——, and S. H. Alemohammad, 2017: Soil moisture retrieval from AMSR-E and ASCAT microwave observation synergy. Part 2: Product evaluation. *Remote Sens. Environ.*, **195**, 202–217, https://doi.org/10.1016/j.rse.2017.04.020.

Koster, R. D., and M. J. Suarez, 2001: Soil moisture memory in climate models. *J. Hydrometeor.*, **2**, 558–570, https://doi.org/10.1175/1525-7541(2001)002<0558:SMMICM>2.0.CO;2.

——, ——, R. W. Higgins, and H. M. Van den Dool, 2003: Observational evidence that soil moisture variations affect precipitation. *Geophys. Res. Lett.*, **30**, 1241, https://doi.org/10.1029/2002GL016571.

——, Coauthors, 2004: Regions of strong coupling between soil moisture and precipitation. *Science*, **305**, 1138–1140, https://doi.org/10.1126/science.1100217.

——, and Coauthors, 2006: GLACE: The Global Land–Atmosphere Coupling Experiment. Part I: Overview. *J. Hydrometeor.*, **7**, 590–610, https://doi.org/10.1175/JHM510.1.

——, Z. Guo, R. Yang, P. A. Dirmeyer, K. Mitchell, and M. J. Puma, 2009: On the nature of soil moisture in land surface models. *J. Climate*, **22**, 4322–4335, https://doi.org/10.1175/2009JCLI2832.1.

——, and Coauthors, 2010: Contribution of land surface initialization to subseasonal forecast skill: First results from a multi-model experiment. *Geophys. Res. Lett.*, **37**, L02402, https://doi.org/10.1029/2009GL041677.

——, Y. Chang, and S. D. Schubert, 2014: A mechanism for land–atmosphere feedback involving planetary wave structures. *J. Climate*, **27**, 9290–9301, https://doi.org/10.1175/JCLI-D-14-00315.1.

Lejeune, Q., E. L. Davin, B. P. Guillod, and S. I. Seneviratne, 2015: Influence of Amazonian deforestation on the future evolution of regional surface fluxes, circulation, surface temperature and precipitation. *Climate Dyn.*, **44**, 2769–2786, https://doi.org/10.1007/s00382-014-2203-8.

LeMone, M. A., F. Chen, M. Tewari, J. Dudhia, B. Geerts, Q. Miao, R. L. Coulter, and R. L. Grossman, 2010a: Simulating the IHOP_2002 fair-weather CBL with the WRF-ARW–Noah modeling system. Part I: Surface fluxes and CBL structure and evolution along the eastern track. *Mon. Wea. Rev.*, **138**, 722–744, https://doi.org/10.1175/2009MWR3003.1.

——, ——, ——, ——, ——, ——, ——, and ——, 2010b: Simulating the IHOP_2002 fair-weather CBL with the WRF-ARW–Noah modeling system. Part II: Structures from a few kilometers to 100 km across. *Mon. Wea. Rev.*, **138**, 745–764, https://doi.org/10.1175/2009MWR3004.1.

Lenschow, D. H., and B. B. Stankov, 1986: Length scales in the convective boundary layer. *J. Atmos. Sci.*, **43**, 1198–1209, https://doi.org/10.1175/1520-0469(1986)043<1198:LSITCB>2.0.CO;2.

Liu, Y. Y., W. A. Dorigo, R. M. Parinussa, R. A. M. de Jeu, W. Wagner, M. F. McCabe, J. P. Evans, and A. I. J. M. van Dijk, 2012: Trend-preserving blending of passive and active microwave soil moisture retrievals. *Remote Sens. Environ.*, **123**, 280–297, https://doi.org/10.1016/j.rse.2012.03.014.

Mahmood, R., and Coauthors, 2014: Land cover changes and their biogeophysical effects on climate. *Int. J. Climatol.*, **34**, 929–953, https://doi.org/10.1002/joc.3736.

Manabe, S., 1969: Climate and the circulation: I. The atmospheric circulation and the hydrology of the Earth's surface. *Mon. Wea. Rev.*, **97**, 739–774, https://doi.org/10.1175/1520-0493(1969)097<0739:CATOC>2.3.CO;2.

McColl, K. A., S. H. Alemohammad, R. Akbar, A. Konings, S. Yueh, and D. Entekhabi, 2017a: The global distribution and dynamics of surface soil moisture. *Nat. Geosci.*, **10**, 100–104, https://doi.org/10.1038/ngeo2868.

——, W. Wang, B. Peng, R. Akbar, D. J. Short Gianotti, H. Lu, M. Pan, and D. Entekhabi, 2017b: Global characterization of surface soil moisture drydowns. *Geophys. Res. Lett.*, **44**, 3682–3690, https://doi.org/10.1002/2017GL072819.

Mei, R., and G. Wang, 2012: Summer land–atmosphere coupling strength in the United States: Comparison among observations, reanalysis data and numerical models. *J. Hydrometeor.*, **13**, 1010–1022, https://doi.org/10.1175/JHM-D-11-075.1.

Mesinger, F., and Coauthors, 2006: North American Regional Reanalysis. *Bull. Amer. Meteor. Soc.*, **87**, 343–360, https://doi.org/10.1175/BAMS-87-3-343.

Milovac, J., K. Warrach-Sagi, A. Behrendt, F. Späth, J. Ingwersen, and V. Wulfmeyer, 2016: Investigation of PBL schemes combining the WRF model simulations with scanning water vapor differential absorption lidar measurements. *J. Geophys. Res. Atmos.*, **121**, 624–649, https://doi.org/10.1002/2015JD023927.

Miralles, D. G., M. J. van den Berg, A. J. Teuling, and R. A. M. de Jeu, 2012: Soil moisture-temperature coupling: A multiscale observational analysis. *Geophys. Res. Lett.*, **39**, L21707, https://doi.org/10.1029/2012GL053703.

——, A. J. Teuling, C. C. van Heerwaarden, and J. V.-G. de Arellano, 2014: Mega-heatwave temperatures due to combined soil desiccation and atmospheric heat accumulation. *Nat. Geosci.*, **7**, 345–349, https://doi.org/10.1038/ngeo2141.

Moeng, C., G. S. Poulos, and M. A. LeMone, 2003: Cooperative Atmosphere–Surface Exchange Study-1999. *J. Atmos. Sci.*, **60**, 2429–2429, https://doi.org/10.1175/1520-0469(2003)060<2429:PCAES>2.0.CO;2.

Muppa, S. K., A. Behrendt, F. Späth, V. Wulfmeyer, S. Metzendorf, and A. Riede, 2016: Turbulent humidity fluctuations in the convective boundary layer: Case studies using water vapour differential absorption lidar measurements. *Bound.-Layer Meteor.*, **158**, 43–66, https://doi.org/10.1007/s10546-015-0078-9.

Notaro, M., 2008: Statistical identification of global hot spots in soil moisture feedbacks among IPCC AR4 models. *J. Geophys. Res.*, **113**, D09101, https://doi.org/10.1029/2007JD009199.

Oke, T. R., 1987: *Boundary Layer Climates*. 2nd ed. Routledge, 435 pp.

Orlowsky, B., and S. I. Seneviratne, 2010: Analysis of land–atmosphere feedbacks and their possible pitfalls. *J. Climate*, **23**, 3918–3932, https://doi.org/10.1175/2010JCLI3366.1.

Pai Mazumder, D., and J. M. Done, 2016: Potential predictability sources of the 2012 U.S. drought in observations and a regional model ensemble. *J. Geophys. Res. Atmos.*, **121**, 12 581–12 592, https://doi.org/10.1002/2016JD025322.

Pan, H.-L., and L. Mahrt, 1987: Interaction between soil hydrology and boundary-layer development. *Bound.-Layer Meteor.*, **38**, 185–202, https://doi.org/10.1007/BF00121563.

Peters-Lidard, C., and L. H. Davis, 2000: Regional flux estimation in a convective boundary layer using a conservation approach. *J. Hydrometeor.*, **1**, 170–182, https://doi.org/10.1175/1525-7541(2000)001<0170:RFEIAC>2.0.CO;2.

Pitman, A. J., and Coauthors, 2009: Uncertainties in climate responses to past land cover change: First results from the LUCID intercomparison study. *Geophys. Res. Lett.*, **36**, L14814, https://doi.org/10.1029/2009GL039076.

Robock, A., K. Ya. Vinnikov, C. A. Schlosser, N. A. Speranskaya, and Y. Xue, 1995: Use of midlatitude soil moisture and meteorological observations to validate soil moisture simulations with biosphere and bucket models. *J. Climate*, **8**, 15–35, https://doi.org/10.1175/1520-0442(1995)008<0015:UOMSMA>2.0.CO;2.

Roundy, J. K., and J. A. Santanello, 2017: Utility of satellite remote sensing for land–atmosphere coupling and drought metrics. *J. Hydrometeor.*, **18**, 863–877, https://doi.org/10.1175/JHM-D-16-0171.1.

——, C. R. Ferguson, and E. Wood, 2013: Temporal variability of land–atmosphere coupling and its implications for drought over the Southeast United States. *J. Hydrometeor.*, **14**, 622–635, https://doi.org/10.1175/JHM-D-12-090.1.

——, ——, and ——, 2014: Impact of land-atmospheric coupling in CFSv2 on drought prediction. *Climate Dyn.*, **43**, 421–434, https://doi.org/10.1007/s00382-013-1982-7.

Santanello, J. A., Jr., M. Friedl, and W. Kustas, 2005: Empirical investigation of convective planetary boundary layer evolution and its relationship with the land surface. *J. Appl. Meteor.*, **44**, 917–932, https://doi.org/10.1175/JAM2240.1.

——, M. Friedl, and M. Ek, 2007: Convective planetary boundary layer interactions with the land surface at diurnal time scales: Diagnostics and feedbacks. *J. Hydrometeor.*, **8**, 1082–1097, https://doi.org/10.1175/JHM614.1.

——, C. D. Peters-Lidard, S. V. Kumar, C. Alonge, and W.-K. Tao, 2009: A modeling and observational framework for diagnosing local land–atmosphere coupling on diurnal time scales. *J. Hydrometeor.*, **10**, 577–599, https://doi.org/10.1175/2009JHM1066.1.

——, ——, and ——, 2011a: Diagnosing the sensitivity of local land–atmosphere coupling via the soil moisture–boundary layer interaction. *J. Hydrometeor.*, **12**, 766–786, https://doi.org/10.1175/JHM-D-10-05014.1.

——, and Coauthors, 2011b: Results from Local Land-Atmosphere Coupling (LoCo) Project. *GEWEX News*, Vol. 21, No. 4, International GEWEX Project Office, Silver Spring, MD, 7–9, www.gewex.org/gewex-content/files_mf/1432209597Nov2011.pdf.

——, S. V. Kumar, C. D. Peters-Lidard, K. Harrison, and S. Zhou, 2013a: Impact of land model calibration on

coupled land–atmosphere prediction. *J. Hydrometeor.*, **14**, 1373–1400, https://doi.org/10.1175/JHM-D-12-0127.1.
——, C. D. Peters-Lidard, A. Kennedy, and S. V. Kumar, 2013b: Diagnosing the nature of land–atmosphere coupling: A case study of dry/wet extremes in the U.S. southern Great Plains. *J. Hydrometeor.*, **14**, 3–24, https://doi.org/10.1175/JHM-D-12-023.1.
——, J. Roundy, and P. A. Dirmeyer, 2015: Quantifying the land–atmosphere coupling behavior in modern reanalysis products over the U.S. southern Great Plains. *J. Climate*, **28**, 5813–5829, https://doi.org/10.1175/JCLI-D-14-00680.1.
Schlosser, C. A., and P. C. D. Milly, 2002: A model-based investigation of soil moisture predictability and associated climate predictability. *J. Hydrometeor.*, **3**, 483–501, https://doi.org/10.1175/1525-7541(2002)003<0483:AMBIOS>2.0.CO;2.
Seneviratne, S. I., and R. D. Koster, 2012: A revised framework for analyzing soil moisture memory in climate data: Derivation and interpretation. *J. Hydrometeor.*, **13**, 404–412, https://doi.org/10.1175/JHM-D-11-044.1.
——, T. Corti, E. L. Davin, M. Hirschi, E. B. Jaeger, I. Lehner, B. Orlowsky, and A. J. Teuling, 2010: Investigating soil moisture–climate interactions in a changing climate: A review. *Earth Sci. Rev.*, **99**, 125–161, https://doi.org/10.1016/j.earscirev.2010.02.004.
——, and Coauthors, 2013: Impact of soil moisture-climate feedbacks on CMIP5 projections: First results from the GLACE-CMIP5 experiment. *Geophys. Res. Lett.*, **40**, 5212–5217, https://doi.org/10.1002/grl.50956.
Song, H.-J., C. R. Ferguson, and J. K. Roundy, 2016: Land–atmosphere coupling at the Southern Great Plains Atmospheric Radiation Measurement (ARM) field site and its role in anomalous afternoon peak precipitation. *J. Hydrometeor.*, **17**, 541–556, https://doi.org/10.1175/JHM-D-15-0045.1.
Stommel, H., 1947: Entrainment of air into a cumulus cloud. *J. Meteor.*, **4**, 91–94, https://doi.org/10.1175/1520-0469(1947)004<0091:EOAIAC>2.0.CO;2.
Tawfik, A. B., and P. A. Dirmeyer, 2014: A process-based framework for quantifying the atmospheric preconditioning of surface triggered convection. *Geophys. Res. Lett.*, **41**, 173–178, https://doi.org/10.1002/2013GL057984.
——, P. A. Dirmeyer, and J. A. Santanello Jr., 2015a: The heated condensation framework. Part I: Description and Southern Great Plains case study. *J. Hydrometeor.*, **16**, 1929–1945, https://doi.org/10.1175/JHM-D-14-0117.1.
——, ——, and ——, 2015b: The heated condensation framework. Part II: Climatological behavior of convective initiation and land–atmosphere coupling over the conterminous United States. *J. Hydrometeor.*, **16**, 1946–196, https://doi.org/10.1175/JHM-D-14-0118.1.
Taylor, C. M., R. A. M. de Jeu, F. Guichard, P. P. Harris, and W. A. Dorigo, 2012: Afternoon rain more likely over drier soils. *Nature*, **489**, 423–426, https://doi.org/10.1038/nature11377.
Teuling, A. J., and Coauthors, 2017: Observational evidence for cloud cover enhancement over western European forests. *Nat. Commun.*, **8**, 14065, https://doi.org/10.1038/ncomms14065.
van den Hurk, B. J. J. M., M. Best, P. Dirmeyer, A. Pitman, J. Polcher, and J. Santanello Jr., 2011: Acceleration of land surface model development over a decade of GLASS. *Bull. Amer. Meteor. Soc.*, **92**, 1593–1600, https://doi.org/10.1175/BAMS-D-11-00007.1.
——, F. Doblas-Reyes, G. Balsamo, R. D. Koster, S. I. Seneviratne, and H. Camargo, 2012: Soil moisture effects on seasonal temperature and precipitation forecast scores in Europe. *Climate Dyn.*, **38**, 349–362, https://doi.org/10.1007/s00382-010-0956-2.
——, and Coauthors, 2016: LS3MIP (v1.0) contribution to CMIP6: The Land Surface, Snow and Soil moisture Model Intercomparison Project—Aims, setup and expected outcome. *Geosci. Model Dev.*, **9**, 2809–2832, https://doi.org/10.5194/gmd-9-2809-2016.
van Heerwaarden, C. C., J. Vilà-Guerau de Arellano, A. F. Moene, and A. A. M. Holtslag, 2009: Interactions between dry-air entrainment, surface evaporation and convective boundary-layer development. *Quart. J. Roy. Meteor. Soc.*, **135**, 1277–1291, https://doi.org/10.1002/qj.431.
——, ——, and A. J. Teuling, 2010: Land-atmosphere coupling explains the link between pan evaporation and actual evapotranspiration trends in a changing climate. *Geophys. Res. Lett.*, **37**, L21401, https://doi.org/10.1029/2010GL045374.
Vinnikov, K. Ya., and I. B. Yeserkepova, 1991: Soil moisture: Empirical data and model results. *J. Climate*, **4**, 66–79, https://doi.org/10.1175/1520-0442(1991)004<0066:SMEDAM>2.0.CO;2.
Vitart, F., and Coauthors, 2017: The Subseasonal to Seasonal (S2S) Prediction project database. *Bull. Amer. Meteor. Soc.*, **98**, 163–176, https://doi.org/10.1175/BAMS-D-16-0017.1.
Wang, S.-Y. S., and Coauthors, 2015: An intensified seasonal transition in the central U.S. that enhances summer drought. *J. Geophys. Res. Atmos.*, **120**, 8804–8816, https://doi.org/10.1002/2014JD023013.
Wei, J., P. A. Dirmeyer, and Z. Guo, 2010: How much do different land models matter for climate simulation?

Part II: A temporal decomposition of land–atmosphere coupling strength. *J. Climate*, **23**, 3135–3145, https://doi.org/10.1175/2010JCLI3178.1.

Williams, I. N., and M. S. Torn, 2015: Vegetation controls on surface heat flux partitioning, and land-atmosphere coupling. *Geophys. Res. Lett.*, **42**, 9416–9424, https://doi.org/10.1002/2015GL066305.

Wulfmeyer, V., and D. Turner, 2016: Land-Atmosphere Feedback Experiment (LAFE) science plan. Rep. DOE/SC-ARM-16-038, 34 pp., www.arm.gov/publications/programdocs/doe-sc-arm-16-038.pdf.

——, and Coauthors, 2015: A review of the remote sensing of lower-tropospheric thermodynamic profiles and its indispensable role for the understanding and the simulation of water and energy cycles. *Rev. Geophys.*, **53**, 819–895, https://doi.org/10.1002/2014RG000476.

——, S. K. Muppa, A. Behrendt, E. Hammann, F. Späth, Z. Sorbjan, D. D. Turner, and R. M. Hardesty, 2016: Determination of convective boundary layer entrainment fluxes, dissipation rates, and the molecular destruction of variances: Theoretical description and a strategy for its confirmation with a novel lidar system synergy. *J. Atmos. Sci.*, **73**, 667–692, https://doi.org/10.1175/JAS-D-14-0392.1.

——, and Coauthors, 2018: A new research approach for observing and characterizing land–atmosphere feedback. *Bull. Amer. Meteor. Soc.*, https://doi.org/10.1175/BAMS-D-17-0009.1, in press.

Xie, S. C., and Coauthors, 2010: ARM climate modeling best estimate data: A new data product for climate studies. *Bull. Amer. Meteor. Soc.*, **91**, 13–19, https://doi.org/10.1175/2009BAMS2891.1.

Yates, D. N., F. Chen, M. A. LeMone, R. Qualls, S. P. Oncley, R. L. Grossman, and E. A. Brandes, 2001: A Cooperative Atmosphere–Surface Exchange Study (CASES) dataset for analyzing and parameterizing the effects of land surface heterogeneity on area-averaged surface heat fluxes. *J. Appl. Meteor.*, **40**, 921–937, https://doi.org/10.1175/1520-0450(2001)040<0921:ACASES>2.0.CO;2.

Zeng, X., M. Barlange, C. Castro, and K. Fling, 2010: Comparison of land–precipitation coupling strength using observations and models. *J. Hydrometeor.*, **11**, 979–994, https://doi.org/10.1175/2010JHM1226.1.

Zhang, J., W.-C. Wang, and J. Wei, 2008: Assessing land-atmosphere coupling using soil moisture from the Global Land Data Assimilation System and observational precipitation. *J. Geophys. Res.*, **113**, D17119, https://doi.org/10.1029/2008JD009807.

Zhang, L., P. A. Dirmeyer, J. Wei, Z. Guo, and C.-H. Lu, 2011: Land–atmosphere coupling strength in the Global Forecast System. *J. Hydrometeor.*, **12**, 147–156, https://doi.org/10.1175/2010JHM1319.1.

Zhang, Y., and S. A. Klein, 2010: Mechanisms affecting the transition from shallow to deep convection over land: Inferences from observations of the diurnal cycle collected at the ARM Southern Great Plains site. *J. Atmos. Sci.*, **67**, 2943–2959, https://doi.org/10.1175/2010JAS3366.1.

NEW SIGNIFICANTLY REVISED TEXTBOOK

AMS EDUCATION

AMS *Ocean Studies* is an introductory, undergraduate-level curriculum package developed, licensed, and nationally implemented by the American Meteorological Society. AMS *Ocean Studies* consists of the new *Ocean Studies: Introduction to Oceanography* textbook, investigations manual, RealTime Ocean Portal, and course management system-compatible files. The 4th edition *Ocean Studies* textbook underwent a major revision with significant updates to content and imagery. It is authored by Douglas A. Segar, Stacy W. Kish, and Elizabeth W. Mills, and includes 15 chapters exploring the world ocean from an Earth system perspective.

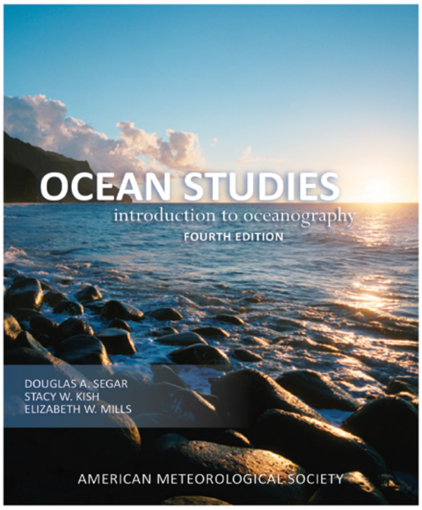

Instructors can use these materials in combinations that cater to face-to-face or online lecture or laboratory courses. Explore the Introductory Chapter of *Ocean Studies* at ametsoc.org/OceanTextbook

A robust, introductory-level oceanography course

Flexible course for undergraduate classrooms

Your adoption of these materials contributes to our ability to provide professional development opportunities in weather, ocean, and climate science to K-12 teachers.

Request a free exam copy at ametsoc.org/OceanStudies

AMS BOOKS

RESEARCH ◆ APPLICATIONS ◆ HISTORY

AMS MEMBERS GET **FREE**

CLIMATE

BEST SELLER!

The Thinking Person's Guide to Climate Change

ROBERT HENSON

This fully updated and expanded revision of The *Rough Guide to Climate Change* combines years of data with recent research. It is the most comprehensive overview of climate science, acknowledging controversies but standing strong in its stance that the climate is changing—and something needs to be done.

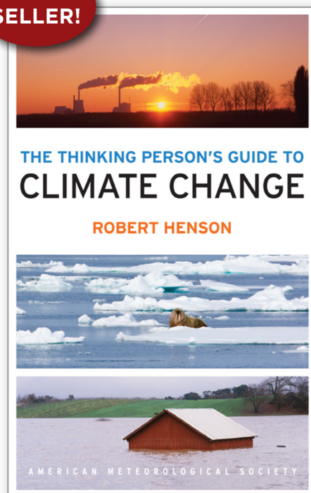

© 2014, PAPERBACK, 520 PAGES,
ISBN: 978-1-935704-73-7
LIST $30 MEMBER $20

Synoptic-Dynamic Meteorology Lab Manual:

Visual Exercises to Complement Midlatitude Synoptic Meteorology

GARY LACKMANN, BRIAN E. MAPES, AND KEVIN R. TYLE

These labs link theoretical concepts with ground-breaking visualization to elucidate concepts taught in the award-winning companion textbook by Gary Lackmann, *Midlatitude Synoptic Meteorology.*

AWARD WINNER!

© 2017, PAPERBACK, 126 PAGES,
ISBN 978-1-878220-26-4
LIST $80 MEMBER $60 STUDENT $50

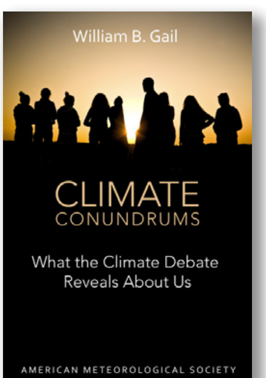

Climate Conundrums:

What the Climate Debate Reveals about Us

WILLIAM B. GAIL

This is a journey through how we think, individually and collectively, about humanity's relationship with nature, and more. Can we make nature better? Could science and religion reconcile? Gail's insights on such issues help us better understand who we are and find a way forward.

© 2014, PAPERBACK, 240 PAGES,
ISBN: 978-1-935704-74-4 LIST $30 MEMBER $20

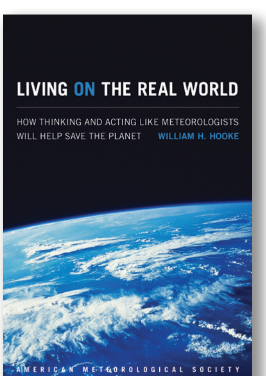

Living on the Real World:

How Thinking and Acting Like Meteorologists Will Help Save the Planet

WILLIAM H. HOOKE

Meteorologists focus on small bits of information while using frequent collaboration to make decisions. With climate change a reality, William H. Hooke suggests we look to the way meteorologists operate as a model for how we can solve the 21st century's most urgent environmental problems.

© 2014, PAPERBACK, 272 PAGES, ISBN 978-1-935704-56-0 LIST $30 MEMBER $22

GUIDES

An Observer's Guide to Clouds and Weather:

A Northeastern Primer on Prediction

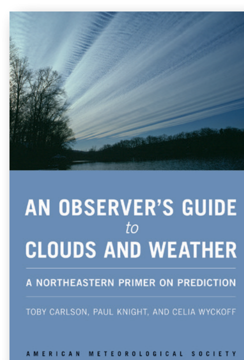

TOBY CARLSON, PAUL KNIGHT, AND CELIA WYCKOFF

With help from Penn State experts, start at the beginning and go deep. This primer, intended for both serious enthusiasts and new meteorology students, will leave you with both refined observation skills and an understanding of the complex science behind the weather: the ingredients for making reliable predictions of your own. It connects fundamental meteorological concepts with the processes that shape weather patterns, and will make an expert of any dedicated reader.

© 2014, PAPERBACK, 210 PAGES,
ISBN: 978-1-935704-58-4 LIST $30 MEMBER $20

Eloquent Science:

A Practical Guide to Becoming a Better Writer, Speaker, and Atmospheric Scientist

DAVID M. SCHULTZ

The ultimate communications manual for undergraduate and graduate students as well as researchers in the atmospheric sciences and their intersecting disciplines.

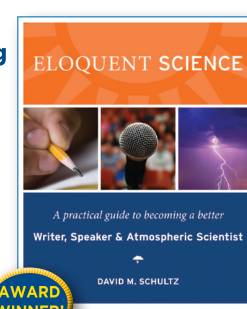

AWARD WINNER!

© 2009, PAPERBACK, 440 PAGES,
ISBN 978-1-878220-91-2
LIST $45 MEMBER $30

To order: bookstore.ametsoc.org, 617-226-3998, or use the order form in this magazine

SHIPPING + DISCOUNTS AT BOOKSTORE.AMETSOC.ORG

NEW

Verner Suomi: The Life and Work of the Founder of Satellite Meteorology

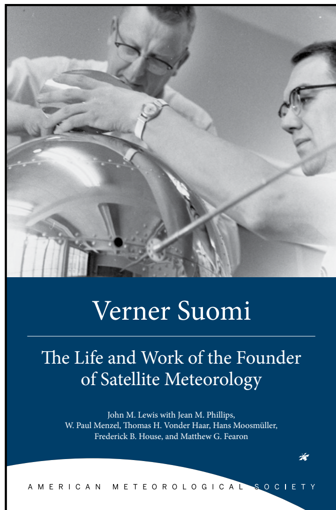

JOHN M. LEWIS WITH JEAN M. PHILLIPS, W. PAUL MENZEL, THOMAS H. VONDER HAAR, HANS MOOSMÜLLER, FREDERICK B. HOUSE, AND MATTHEW G. FEARON

Born in a Minnesotan mining town, Suomi would spend his best years next door in Wisconsin, but not before seeing the whole world—from space, that is. This is the story of the scientist, inventor, and teacher who founded satellite meteorology, written by members of the communities that grew up around his groundbreaking work.

LIST $30 MEMBER $20

© 2016, PAPERBACK, 240 PAGES, ISBN: 978-1-944970-22-2

Weather in the Courtroom: Memoirs from a Career iForensic Meteorology

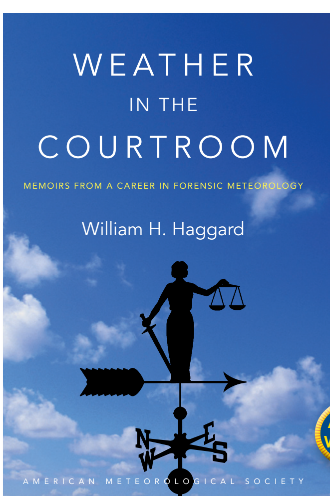

AWARD WINNER!

WILLIAM H. HAGGARD

From a pioneering forensic meteorologist, the inside scoop on legendary litigations, including the disappearance of an Alaskan congressman's airplane in 1972, the collapse of Tampa Bay's Skyway Bridge in 1980, and the crash of Delta Flight 191 in Dallas/Fort Worth in 1985.

LIST $30 MEMBER $20

© 2016, PAPERBACK, 240 PAGES, ISBN: 978-1-940033-95-2

AMS American Meteorological Society

Booksellers, groups, or for examination copies:
The University of Chicago Press:
1-800-621-2736 (US & Canada)
773-702-7000 (all others)
custserv@press.uchicago.edu

HISTORY

Taken by Storm, 1938: A Social and Meteorological History of the Great New England Hurricane, 2nd Ed.

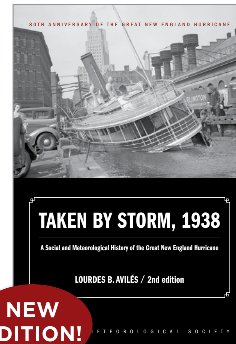

NEW EDITION!

LOURDES B. AVILÉS

80TH ANNIVERSARY OF *STORM*

The science behind the 1938 Hurricane, which hit New England unannounced, is presented here for the first time along with new data that sheds light on the motivations of the Weather Bureau forecasters. This compelling history successfully weaves science, historical accounts, and social analyses to create a comprehensive picture of the most powerful and devastating hurricane to hit New England to date.

© 2018, PAPERBACK, 288 PAGES, ISBN: 978-1-944970-24-6

LIST $30 MEMBER $20

A Scientific Peak: How Boulder Became a World Center for Space and Atmospheric Science

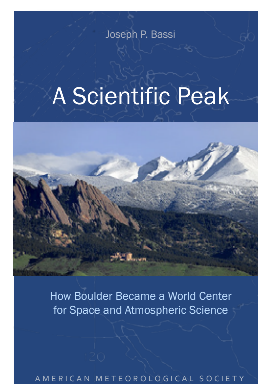

JOSEPH P. BASSI

How did big science come to Boulder, Colorado? Joe Bassi introduces us to the characters, including Harvard sun–Earth researcher Walter Orr Roberts, and the unexpected brew of politics, passion, and sheer luck that during the Cold War era transformed this "Scientific Siberia" to home of NCAR and NOAA.

© 2015, PAPERBACK, 264 PAGES, ISBN: 978-1-935704-85-0

LIST PRICE: $35.00 MEMBER PRICE: $25.00

Hurricane Pioneer: Memoirs of Bob Simpson

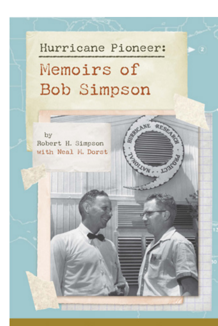

ROBERT H. SIMPSON AND NEAL DORST

In 1951, Bob Simpson rode a plane into a hurricane—just one of the many pioneering exploits you'll find in these memoirs. Bob and his wife Joanne are meteorological icons: Bob was the first director of the National Hurricane Research Project and a director of the National Hurricane Center. He helped to create the Saffir–Simpson Hurricane Scale; the public knows well his Categories 1–5. Proceeds from this book help support the AMS's K. Vic Ooyama Scholarship Fund.

© 2015, PAPERBACK, 156 PAGES
ISBN: 978-1-935704-75-1 **LIST $25 MEMBER $20**